SHUTTLE S-BAND COMMUNICATIONS TECHNICAL CONCEPTS

J. W. Seyl, W. W. Seibert, J. A. Porter, D. S. Eggers,
S. W. Novosad, H. A. Vang, S. D. Lenett, W. A. Lewton,
and J. F. Pawlowski
NASA Lyndon B. Johnson Space Center
Houston, Texas 77058

ABSTRACT

The Shuttle S-band communications system provides the Shuttle Orbiter with the capability to communicate directly with the Earth by way of the Ground Spaceflight Tracking and Data Network (GSTDN) or by way of the Tracking and Data Relay Satellite System (TDRSS), which relays Orbiter information signals through a geosynchronous satellite to/from the Earth. S-band frequencies provide the primary links for direct Earth and TDRSS communications during all launch and entry/landing phases of Shuttle missions. While on orbit, the Orbiter uses its S-band links when TDRSS K_u-band is not available, when conditions require Orbiter attitudes unfavorable to K_u-band communications, or when the payload bay doors are closed. The Shuttle S-band communications functional requirements, the Orbiter hardware configuration, and the NASA S-band communications network are described. The requirements and implementation concepts which resulted in new or unique techniques for Shuttle S-band hardware development are discussed. These areas include (1) digital voice delta modulation, (2) convolutional coding/Viterbi decoding, (3) critical modulation index for phase modulation using a Costas loop (phase-shift keying) receiver, (4) optimum digital data modulation parameters for continuous-wave frequency modulation, (5) intermodulation effects of subcarrier ranging and time-division multiplexing data channels, (6) radiofrequency coverage, and (7) despreading techniques under poor signal-to-noise conditions. The performance of these new and unique communication channels is reviewed, with analytical and experimental results of performance provided.

INTRODUCTION

The Shuttle functional communication requirements are met through the use of three basic communication network modes. The NASA Ground Spaceflight Tracking and Data Network (GSTDN) mode provides for communication links from the Shuttle to the NASA network ground stations. The U.S. Air Force (USAF) Space Ground Link System (SGLS) mode provides for communication to the Air Force Satellite Control Facility (AF/SCF) by way of a remote tracking site (RTS). The NASA Tracking and Data Relay Satellite (TDRS) mode provides for communication links from the Shuttle to a geosynchronous orbiting satellite for relay to the NASA White Sands Ground Terminal. These S-band links represent the primary communication capability of the Shuttle for all mission phases when the TDRS K_u-band communication link is not available. All Shuttle missions through STS-6 depended solely on the NASA GSTDN and/or the AF/SCF SGLS S-band communication modes.

Figure 1 illustrates the communication links associated with the Shuttle S-band modes. Each mode uses a common Orbiter network subsystem, which is also shown functionally in figure 1. Table 1 defines the link capabilities, the modulation techniques employed, and unique design features. The frequencies for each of the S-band communication modes are given in table 2. The SGLS mode uplink is actually in the L-band frequency range for compatibility with the AF/SCF RTS transmitters.

To provide the multiple functions such as two duplex voice channels and command data on the uplinks, a time-division multiplexing (TDM) technique is incorporated. Similarly, TDM is used on the downlinks to allow simultaneous transmission of two duplex voice channels and telemetry data on a single carrier signal.

To achieve optimum performance on these digital channels, a phase modulation (PM) system was developed. In addition, a frequency-modulated (FM) channel is provided for transmission of television or other analog/digital data which cannot be handled by the PM links. The PM link used for communications through the Tracking and Data Relay Satellite can operate at two digital data rates. The low-data-rate mode is provided to ensure adequate link margins if communication channel parameters operate near their worst case tolerances. When operating through the TDRS, the phase modulation index is optimized at ±90°, which is referred to as phase-shift keying (PSK).

An important characteristic of the S-band links is the coverage provided by the S-band PM switched-beam antennas, which are flush mounted at four locations on the Shuttle vehicle. These antennas allow nearly continuous communication when a network element is visible, without requiring Shuttle attitude constraints.

The Shuttle S-band GSTDN network (fig. 2) consists of 13 NASA ground stations and 2 USAF AF/SCF
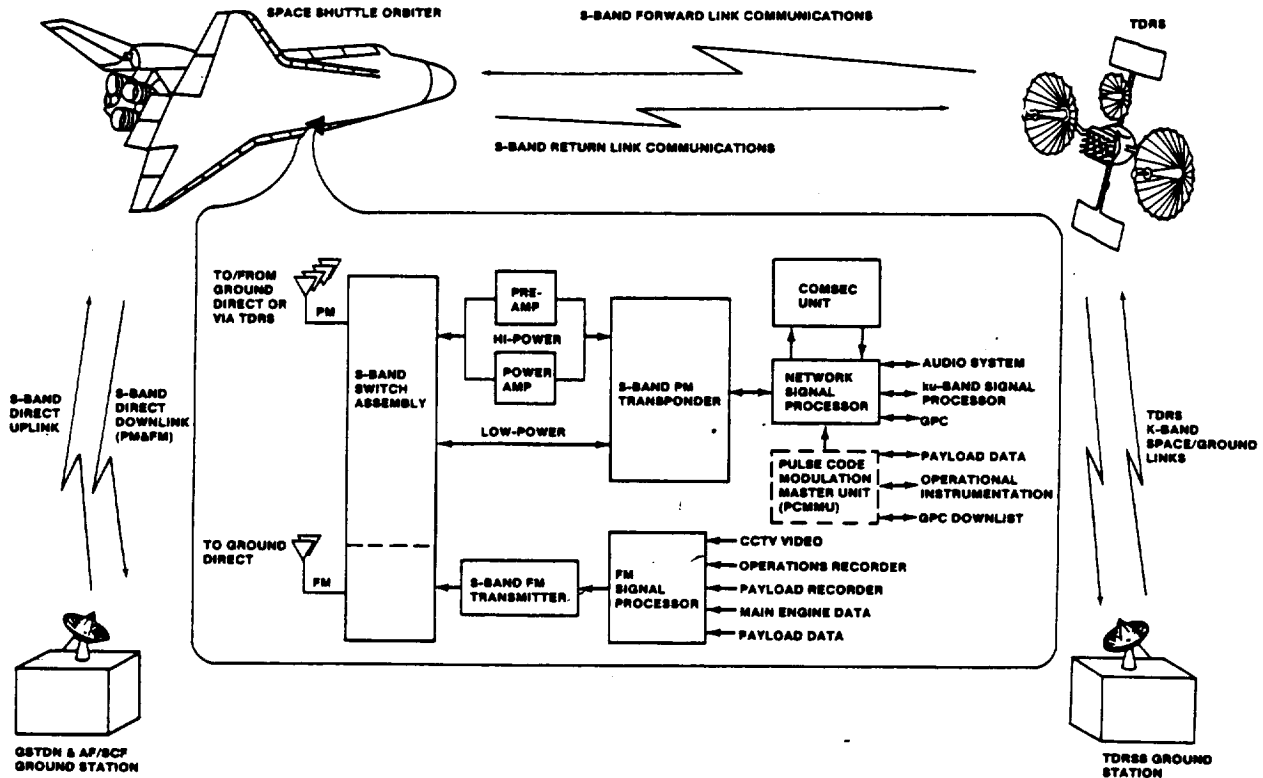
FIGURE 1.- ORBITER OPERATIONAL S-BAND SYSTEM.

remote sites. The TDRS system (TDRSS) is scheduled to be available after STS-6. The TDRSS network (fig. 2) consists of two satellites and a spare satellite. The TDRSS network will provide significantly more coverage than previously available. When the TDRSS is operational, the number of NASA ground stations will be reduced and only those necessary to cover launch and landing phases will be retained for Shuttle support.

In the following sections, the S-band communication modes are discussed in detail. The unique techniques and designs incorporated in the Orbiter S-band network hardware to provide these links are highlighted. Performance characteristics, including the effects of nonideal hardware parameters for links that incorporate new or advanced communication concepts, are reviewed.

TRACKING AND DATA RELAY SATELLITE SYSTEM MODE TECHNIQUES

To communicate with the Earth by way of the TDRS, the Shuttle S-band network subsystem design incorporated several new and sophisticated techniques. Many of these techniques are necessary to enhance the channel performance for adequate circuit margins, whereas some resulted from operational requirements and constraints.

To optimize performance and to provide a secure communications capability, an all-digital link design emerged. Thus, a method for digitizing voice and multiplexing the voice and data channels was required. To maintain the data rate as low as possible for link margin purposes, a delta modulation process was selected for voice digitizing. This technique allows the minimum number of bits (one) to be used for each voice sample. In addition, the voice sampling rate was reduced to as low a value as practical consistent with good quality. Two modes are provided for the TDRSS links. In mode 2, two duplex voice channels are available, each operating at a 32-kbps sample rate on the forward and return links. In mode 1, a single duplex voice channel is available. The forward link sample rate is reduced to 24 kbps, whereas the return link sample rate is maintained at 32 kbps.

Even with the efforts to minimize the required data rates for the forward and return links, other factors eventually forced incorporation of convolutional coding to achieve the needed performance. For example, communications through the TDRS must be maintained independent of Shuttle attitude. This requirement dictates use of relatively broad beam, low-gain antennas to maximize the

721

TABLE 1.- SHUTTLE S-BAND COMMUNICATIONS LINK CAPABILITIES, MODULATION TECHNIQUES,
AND UNIQUE FEATURES

Frequency	Communications link	Capability	Modulation technique	Unique features
S-band (Hi-Lo)	Orbiter-GSTDN downlink	Telemetry (Hi-Lo data rates) Voice (1 or 2 channels) Ranging Doppler (2-way)	Phase modulation (PM)	Linear PM baseband data with ranging on 1.7-MHz subcarrier
S-band	Orbiter-GSTDN downlink	Payload data Recorded data Operational Payload Television	Frequency modulation (FM)	FM deviation optimized for maximum digital data rates
S-band (Hi-Lo)	GSTDN-Orbiter uplink	Command Voice (1 or 2 channels) Ranging	PM or phase-shift keyed (PSK)	Linear PM baseband data with ranging on 1.7-MHz subcarrier
S-band (Hi-Lo)	Orbiter-TDRSS return link	Telemetry (Hi-Lo data rates) Voice (1 or 2 channels) Doppler (2-way)	PSK	Convolutional encoding rate 1/3, Viterbi decoding
S-band (Hi-Lo)	TDRSS-Orbiter forward link	Command Voice (1 or 2 channels)	PSK/spread spectrum	Spread spectrum to meet CCIR rqmts, TDM convolutional encoded rate 1/3, Viterbi decoding
S-band (Hi-Lo)	Orbiter-AF/SCF downlink	Telemetry (Hi-Lo data rates) Voice (1 or 2 channels) Doppler (2-way)	PM	Secure links, telemetry and voice
S-band	Orbiter-AF/SCF downlink	P/L data (real-time) Recorded data Operational Payload	FM	Secure data links
S-band (Hi-Lo)	AF/SCF-Orbiter uplink	Command Voice (1 or 2 channels)	PM	Secure command and voice links

radiofrequency (rf) coverage. A network of four (quad) antennas flush mounted on the Shuttle fuse-lage with computer-driven switching logic is used to accomplish the needed coverage. As a result of these antenna characteristics, the transmitter power and receiver sensitivity had to be pushed to state-of-the-art values. A 140-watt power amplifier (traveling-wave tube (TWT)) was developed by Watkins-Johnson, and a receiver with less than a 3.0-decibel noise figure was developed by TRW. Even with these state-of-the-art rf components, convolutional encoding was necessary to achieve adequate link performance margins. A nontransparent rate one-third code with constraint length of 7 was selected. The decoding algorithm used was that developed by A. J. Viterbi (ref. 1); it has been shown to be optimum in the maximum likelihood sense.

The modulation process was also selected on the basis of optimizing the channel performance; hence, PSK was chosen. A Costas loop provides for carrier reconstruction and data recovery of both forward and return link signals.

TABLE 2.- SHUTTLE S-BAND MODE FREQUENCIES

Communications mode	S-band frequencies, MHz	
	Uplink/forward link	Downlink/return link
GSTDN - high frequency	2106.4063	2287.5
GSTDN - low frequency	2041.9479	2217.5
AF/SCF - SGLS - high frequency	1831.7870	2287.5
AF/SCF - SGLS - low frequency	1776.7330	2217.5
TDRSS - high frequency	2106.4063	2287.5
TDRSS - low frequency	2041.9479	2217.5

Because the TDRS satellites continuously radiate the Earth with S-band energy, the forward link S-band signal power flux density in a 4-kilohertz bandwidth must be maintained below the level consistent with international agreements. To meet this requirement, a pseudorandom code is used to spread the TDRS-transmitted energy over a significantly larger bandwidth than would normally be required for the information rates involved. This technique of "spread spectrum" modulation greatly increases the complexity of the Shuttle S-band TDRS receiver, since a despread version of the information signal must be developed before the data can be recovered with conventional phase-lock loop techniques. The following paragraphs describe these new and unique techniques resulting from the TDRSS communications mode requirements.

DIGITAL VOICE/TIME-DIVISION MULTIPLEXING

There are two reasons for including a digital (TDM) link in the Shuttle Program. The first is that the use of the TDRSS for NASA missions provides a high rf coverage capability but results in relatively weak S-band links. Analog signal designs could not provide adequate margins, but digital links with channel coding can. The second reason for use of a digital TDM link is to satisfy the requirement for message privacy.

The Shuttle system incorporated a signal design in which one or two digitized speech channels are time-division multiplexed with commands or telemetry. The composite data stream is convolutionally encoded prior to rf transmission. This approach is more efficient than analog since no power is wasted in unrecoverable intermodulation products and a substantial reduction in rf power is achieved using error correction coding.

Digitizing of Shuttle voice is accomplished by delta modulation techniques. Figure 3 is a simplified functional diagram of the delta modulation process. Also illustrated are the analog input and resulting digital output signals. In the modulation process, the input analog signal's instantaneous value is digitized according to a particular algorithm. Based on the generated data (bit) stream, the step size processor and feedback device reproduces the analog input $\hat{m}(t)$ for comparison with the actual input signal $m(t)$. If $\hat{m}(t) < m(t)$, then a binary one output results. If $\hat{m}(t) > m(t)$, then a binary zero output results. In the demodulation process, the data (bit) stream is the input to the step size processor and the feedback portion of the demodulator, which then reproduces a replica of the original input analog signal. The output is filtered to smooth the samples and remove unwanted noise components which may result from the delta modulation processing.

Delta modulation is employed on the Shuttle because it provides approximately the same voice intelligibility as pulse code modulation (PCM), but at one-half the bandwidth. Delta modulation is intelligible, with speaker recognition and bit error rates as low as 10^{-1} for some adaptive delta modulation (ADM) techniques. Several ADM algorithms were tested by NASA to select one that would maintain high word intelligibility with reasonable voice quality at sampling rates of 32 or 24 kbps in the presence of very high channel errors (i.e., bit error rates approximately 10^{-1}). The delta modulation algorithm selected by NASA to satisfy these requirements is a modified version of the "ABATE" algorithm (ref. 2).

The TDRSS link margins are small, and convolutional encoding is used for efficient operation. The errors for such a coded channel will exhibit a burst characteristic. The need to maintain voice communications as long as possible in a burst-error environment was a key factor in the selection of the "Modified ABATE" algorithm. The Modified ABATE algorithm equation is illustrated in figure 4.

The unique feature of the Modified ABATE algorithm is that it was designed to adaptively follow the received signal with an extremely high channel error rate (approximately 10^{-1}). When an error

FIGURE 2.- SHUTTLE S-BAND NETWORK (GSTDN, AF/SCF, AND TDRSS).

ACN - ASCENSION ISLAND
AGO - SANTIAGO, CHILE
BDA - BREMUDA
BOT - BOTSWANA
BUC - BUCKHORN, CA
DKR - DAKAR, SENEGAL

GDS - GOLDSTONE, CA
GWM - GUAM
HAW - HAWAII
IOS - INDIAN OCEAN
MAD - MADRID, SPAIN
MIL - MILA AND PONCE DELEON, FL

ORR - ORRORAL VALLEY, AUSTRALIA
VTS - VANDENBERG AFB
YAR - YARGADEE, AUSTRALIA

(PERCENTAGE COVERAGE FOR A TYPICAL SHUTTLE MISSION:
GSTDN ~ 15%, TDRSS ~ 80%)

occurs in the received data stream, the step size processor will produce erroneous step sizes until a correctly received data transition is detected. The average number of erroneous step sizes following a received error in the Modified ABATE algorithm is less than in other popular ADM algorithms (ref. 3). It is this feature that gives the Modified ABATE algorithm its good performance in the presence of channel errors. The Modified ABATE algorithm sounds significantly better at an error rate of 10^{-1} than do other ADM algorithms. This improved error performance is obtained at the expense of frequency response and dynamic range.

The ADM is relatively immune to channel errors whether they occur randomly or in bursts. Some of the results obtained by NASA from word-intelligibility tests of the Modified ABATE algorithm are summarized in table 3. The burst errors scored in table 3 were limited to burst lengths of 10 bits. These bursts occurred randomly, but, during a burst, the probability of error was 0.5. The bit error rate (BER) presented in table 3 is the average error rate. Note that the ADM is more immune to burst errors than to random errors. Figure 5 shows word intelligibility as a function of BER for random

724

VOLTAGE

m(t)

TIME

1 1 1 0 0 0 0 1 0 ...

e(t)   1 1 1 0 0 0 0 1 0 ... t

FROM INFORMATION SOURCE   +

$\stackrel{\wedge}{m(t)}$

```
                          ┌──────────────┐
                     +    │  COMPARATOR  │────○────── TO CARRIER MODULATOR
                     −    └──────────────┘    │
                                              │
                                              ▼
                                      ┌──────────────┐
                                      │  STEP SIZE   │
                                      │  PROCESSOR   │
                                      └──────────────┘
                                              │
                      ┌──────────────┐        │
                      │   FEEDBACK   │◄───────┘
                      │    DEVICE    │
                      │   AND D/A    │  S(t)
                      └──────────────┘
```

FIGURE 3.- DELTA MODULATION PROCESS.

m (t)

$\stackrel{\wedge}{m}$(t)

$\frac{\div}{\top}$ S$_o$ = MINIMUM STEP SIZE

e (t) = 1 1 1 1 1 1 1 1 0 0 0 1 1 0 1 0 1 0   t

$$S(t+1) \begin{cases} [|S(t)| + S_o] \ e(t) \ ; \ \text{WHEN} \ e(t) = e(t-1) \ \text{AND} |S(t)| < 8 \ S_o \\ |S(t)| \ e(t) \ ; \ \text{WHEN} \ e(t) = e(t-1) \ \text{AND} |S(t)| = 8 \ S_o \\ |S_o| \ e(t) \ ; \ \text{OTHERWISE I.E.} \ e(t) \neq e(t-1) \end{cases}$$

FIGURE 4.- MODIFIED ABATE ADAPTIVE DELTA MODULATION ALGORITHM.

725

TABLE 3.- PERFORMANCE OF THE MODIFIED ABATE ALGORITHM

Sampling rate, kbps	Bit error type	Bit error rate	Word-intelligibility score
32	Random	3.5×10^{-5} 2.7×10^{-2} 1.3×10^{-1}	96.5 95.2 76.1
16	Random	4.6×10^{-5} 1.7×10^{-2} 8.8×10^{-2}	95.1 93.6 88.8
32	Burst	9.2×10^{-5} 2.3×10^{-2} 1.5×10^{-1}	94.7 94.7 87.5

FIGURE 5.- MEASURED WORD INTELLIGIBILITY FOR RANDOM BIT ERRORS - MODIFIED ABATE DELTA MODULATION ALGORITHM.

errors (i.e., not burst errors) resulting from Shuttle voice channel verification tests performed in the NASA Lyndon B. Johnson Space Center (JSC) Electronic Systems Test Laboratory (ESTL) (ref. 4).

Word intelligibility of 87.5 percent with an average BER of 1.5×10^{-1} can be achieved with burst errors. The word-intelligibility results in table 3 and figure 5 were achieved using postdemodulation band-pass filtering (300 to 2300 hertz). The delta demodulator is essentially an integrator; thus, its output noise power spectrum is approximately kf^{-2}, where k is a constant the value of which depends on the BER. The 300-hertz high-pass filter was used to eliminate a large portion of this low-frequency noise due to channel errors. The 2300-hertz low-pass filter was chosen to eliminate the higher frequency components due to sampling.

CONVOLUTIONAL CODING/VITERBI DECODING

Because of the long range to the TDRS (geosynchronous orbit) and the Shuttle's antenna characteristics, the required performance for the Shuttle/TDRSS links could not be achieved by brute force methods, i.e., by increased transmitter power and reduced receiver noise temperatures. In fact, even with the 140-watt Shuttle transmitter power, and a low-noise parametric amplifier receiver, the forward and return TDRSS links required error correction channel encoding to achieve the design goal BER performance.

A simplified functional diagram for a digital communication channel is shown in figure 6. Because the received data bit is corrupted with noise, a finite probability of error exists in the bit decision process. For a PSK-modulated channel assuming optimum matched-filter detection, the probability of error at the receiver has been shown to be

$$Pe = \frac{1}{2} \, erfc \, \sqrt{\frac{E_c}{N_0}} \tag{1}$$

where E_c is the signal energy of a channel bit at the input to the decision device, N_0 is the noise spectral density of the receiver system, and erfc is the complementary error function.
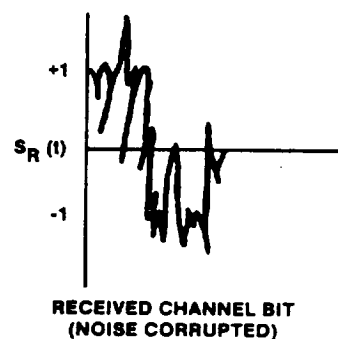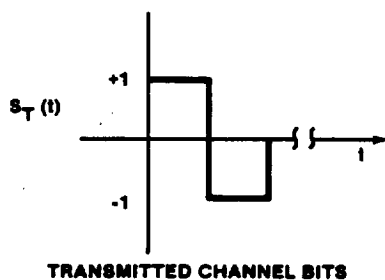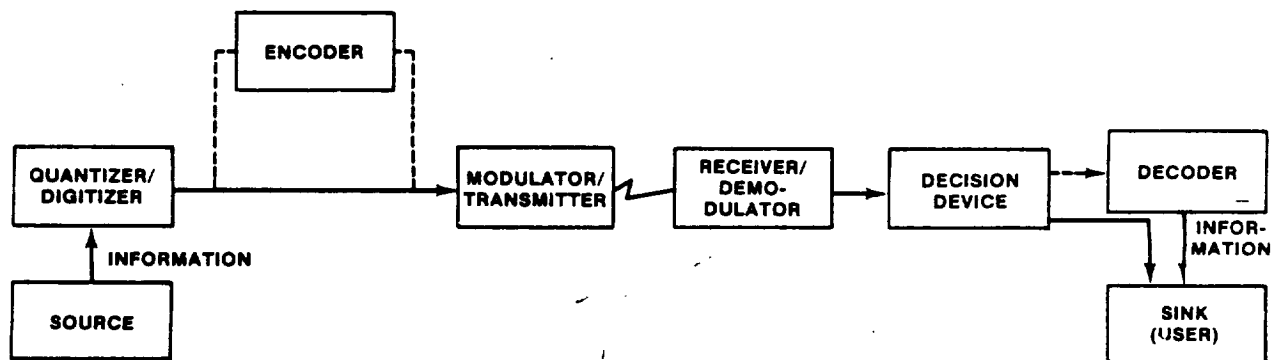
FIGURE 6.- FUNCTIONAL BLOCK DIAGRAM OF A DIGITAL COMMUNICATION CHANNEL.

If coding is not employed, the received bit is directly equivalent to the transmitted bit. The receiver bit decision is thus made on information bits directly. If transmitted and received power is held constant for coded and uncoded channels, then more energy is available for decisions on information bits than for decisions on channel bits (symbols), since each information bit is represented by two or more symbols. This redundancy results in lower energy-to-noise density ratios for the coded symbols and hence a higher error rate. The decoder's task is to correct as many of these bit errors as possible resulting in a net coding gain. For coding gain to be achieved, the information BER must be less after decoding than it would have been for an uncoded channel.

The choice of coding parameters selected for the Orbiter/TDRSS link was the culmination of a series of trade studies, hardware constraints, link margins, and empirical tests. It is well documented that convolutional codes can outperform block codes with comparable decoding hardware. The decision then centered upon selecting either a sequential decoder or a Viterbi decoder and their associated rates and constraint lengths.

Use of coding was dictated by link margin considerations, and the design goal was to improve channel performance by 4 to 5 decibels. Since voice quality could be maintained with error rates on the order of 10^{-1}, the overall communication link had to be designed to ensure a graceful degradation of the system to prevent premature loss of voice communications.

The decoding of convolutional codes is by far a more complex operation than encoding. Since size, weight, and power are at a premium on the Orbiter, a study of the complexity of both sequential and Viterbi decoders was conducted for the maximum uplink data rate of 72 kbps. The complexity of the decoder is a function of the rate of the code, the constraint length, the quantization of the demodulated data bits, and the required output BER. It was found that as the code rate is decreased and the quantization is increased, the Viterbi decoder performance for a given complexity improves in relation to the sequential decoder. In addition, at the BER crossover point, the Viterbi decoder degrades gracefully but the sequential decoder does not. For the link robustness, ease of resynchronization, and relative insensitivity to data bit quantization, the Viterbi decoder was chosen.

The coding gain of the Viterbi decoder at a BER of 1×10^{-5} can roughly be summarized as follows, for constraint lengths on the order of 3 to 8. The coding gain improves roughly 0.5 decibel for every increase in the constraint length. An increase of 2 decibels in coding gain can be obtained by increasing the symbol bit decision quantization from 2 to 8 levels (i.e., soft decision compared to hard decision performance improvement). Another 0.5 decibel gain can be achieved by decreasing the code rate from one-half to one-third. The Viterbi decoder complexity at these data rates roughly doubles with each increase in constraint length. The design goal of 5 decibels coding gain could have been achieved with a rate one-half, constraint length 7 code. However, an additional 0.4 decibel coding gain was achieved by changing the code rate from one-half to one-third. This change in code rate did not significantly affect decoder complexity.

The symbol synchronization performance is critical in a coded communication system in which large coding gains are expected. This coding gain corresponds to a reduction in the energy per symbol to noise spectral density available for symbol synchronization and detection. To achieve the expected coding gains, the symbol synchronizer must introduce negligible degradation. The Shuttle channel coding that was selected is the rate one-third, constraint length 7 code. Since there is still intelligible voice at BER's of 10^{-1}, the symbol synchronizer must still operate properly at this error rate. This requirement forces the symbol synchronizer to acquire and lock at approximately -5 decibels E_c/N_o, which was met with a digital implementation of the symbol synchronizer to ensure repeatable and reliable operation.

The Viterbi decoder implements a maximum likelihood algorithm to estimate the transmitted data bit. To save hardware, the algorithm performs 2^{K-1} decisions every bit time, where K is the constraint length of the system. With timing overhead, the decoder must perform an operation every 190 nanoseconds for a constraint length equal to 7. This is the limit at which the hardware can process data with the logic family selected (low-power Schottky). The Orbiter Viterbi decoder implementation provides a coding gain of 5.4 decibels at a BER of 1×10^{-5}. Figure 7 illustrates the theoretical performance improvement of the Shuttle convolutional encoded, Viterbi decoded channel over the optimum PSK uncoded channel (ref. 5).

SPREAD SPECTRUM MODULATION

The application of spread spectrum techniques to communications systems provides several capabilities which cannot be obtained with conventional techniques. Some of the capabilities for which spread spectrum techniques are commonly adapted include antijamming, multiple-access communication, message privacy, and navigation. In most of these applications, the ratio of the spreading chip rate to the information data rate is large (>10^3) and the signal-to-noise ratio (SNR) in the information rate bandwidth is high (>10 decibels). For the Shuttle Orbiter application, the spreading process is

728
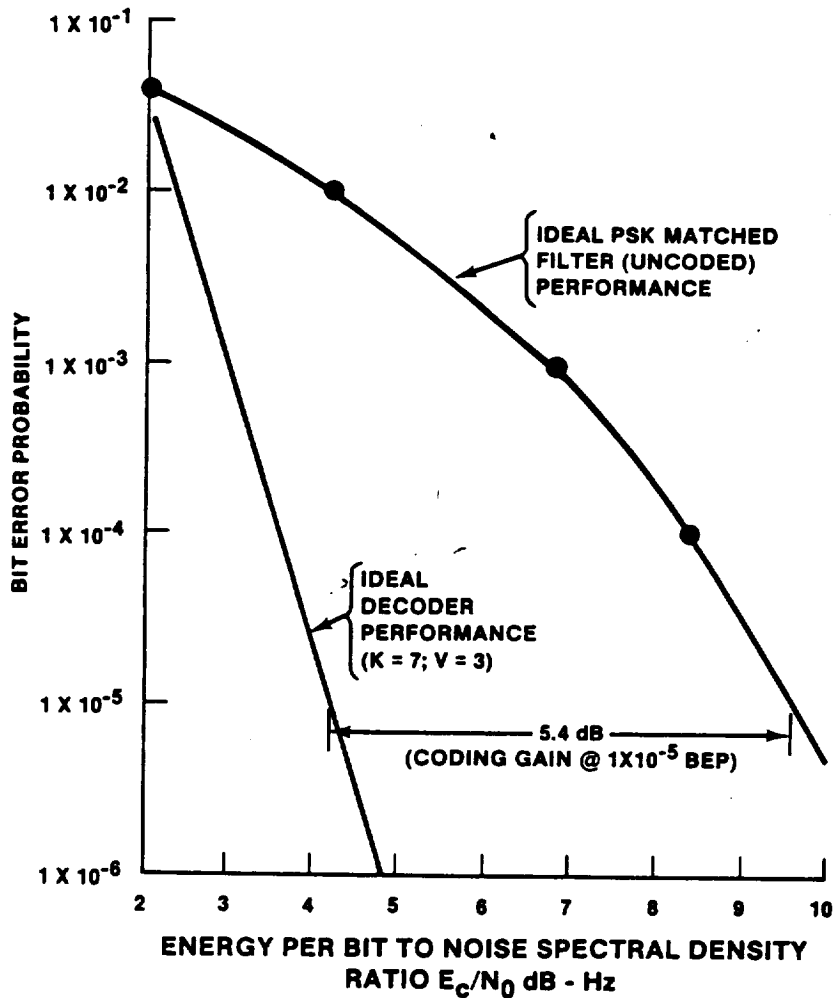
FIGURE 7.- BIT ERROR PROBABILITY PERFORMANCE
IMPROVEMENT FOR IDEAL CODED CHANNEL.

used to reduce the rf power spectral density. For this case, the spreading chip rate is purposely se-
lected as low as possible to just meet the required power spectral density levels. Hence, the ratio
of spreading chip rate to information rate is considerably less than that normally encountered. In
addition, the information is Manchester encoded,, and an information bandwidth of approximately twice
the data rate is required for the despreading process. These factors, together with operations re-
quired at SNR's close to 0 decibel in the information bandwidth, make the Shuttle Orbiter despreading
system design unique.

The International Radio Consultative Committee (CCIR) of the International Telecommunication
Union (ITU) recommends various criteria concerning rf signals and their spectra. The rf frequency
bands currently used by commercial communications satellites are the same as those used by the common
carriers for microwave relay systems on Earth. To allow frequency sharing, various criteria are
established by CCIR to prevent mutual interference. Many studies were made by international experts
on the subject, and several recommendations have resulted. One particular item specifies the maximum
allowable power flux density received at the Earth's surface from an Earth-orbiting satellite (space
station). The power flux density is defined by

$$F = EIRP/4\pi d^2 \qquad (2)$$

729

where

      $\bar{F}$ = flux density
   EIRP = effective isotropic radiated power
      d = distance between spacecraft and Earth in meters

    Table 4 presents the maximum allowable power flux density at the Earth's surface from an Earth-orbiting satellite for the Shuttle Orbiter S-band frequency. The values tabulated show that the most stringent requirements occur for signals having an angle of incidence above the horizontal plane of $0°$ to $5°$ and indicate how the flux-density requirements vary as a function of the angle of arrival of the rf signal.

    The TDRS to Shuttle Orbiter S-band forward communication link would exceed the CCIR requirements without additional modulation to spread the flux density over a much larger bandwidth. Thus, a spread spectrum signal design was developed for Shuttle to maintain compliance with the CCIR requirements on flux density. In the spread spectrum concept, the signal spectrum is expanded at the transmitter before transmission. This expansion distributes the signal energy over a bandwidth much greater than the information bandwidth normally required. The spreading technique chosen for Shuttle involves direct-sequence, pseudorandom code biphase modulation of the information carrier signal. Figure 8 is a simplified block diagram of a spread spectrum system using pseudonoise (PN) code modulation.

<div align="center">TABLE 4.- CCIR FLUX-DENSITY GUIDELINES</div>

Frequency band	Maximum flux density in 4-kHz bandwidth, dBW/m^2, for angle of arrival (δ) above the horizontal plane of -		
	$0°$ to $5°$	$5°$ to $25°$	$25°$ to $90°$
S-band	-154.0	$-154 + \dfrac{\delta - 5°}{2}$	-144

    The rf carrier which is modulated with the data signal of rate R_d is passed to a balanced PSK modulator. The PN code generator supplies a binary sequence of ones and zeros to the PSK modulator. Typically, a binary "1" is sent as unperturbed carrier phase, whereas a binary "0" is sent by a change in phase of the carrier of $180°$. This process has the effect of "spreading" the signal over a bandwidth roughly equal to twice the rate of the PN code (R_c). The resulting spread signal is then transmitted over the communication channel. At the receiver, after downconverting to a suitable intermediate frequency (i.f.), an identical PN code is correlated with the received code. After despreading, only the original data modulation remains and is passed to a conventional PSK demodulator. Other (interfering) signals received will not be correlated and are effectively spread by the receiver PN code, thus appearing as noise to the data demodulator. Figure 9 is a sketch of typical spectra for the transmitted and received signals at various points in the system as indicated by the circled numbers in figures 8 and 9.

    If a uniformly distributed, transmitted spread spectrum is assumed, it can be shown that the spreading code rate must satisfy equation (3) (ref. 6).

$$10 \log R \geq \mathrm{EIRP}|_{dBW} + \log B/2 - 22 \ dB - 20 \log d - \mathrm{CCIR}|_{dBW/m^2/Hz} \qquad (3)$$

where

               R = the spreading code rate
      $\mathrm{EIRP}|_{dBW}$ = the satellite transmitted EIRP in decibels referenced to 1 watt
             B = measurement bandwidth (4 kilohertz for CCIR requirement)
             d = range from the satellite to the Earth surface in meters
  $\mathrm{CCIR}|_{dBW/m^2/Hz}$ = CCIR power flux-density requirement

    For the case of the TDRS in geosynchronous orbit and assuming the worst case CCIR requirement for less than $5°$ elevation angles, the Shuttle minimum spreading code rate is 10.7 Mbps for the S-band forward link. The actual S-band spreading code rate is 11.232 Mbps, and the code length is 2047 chips.
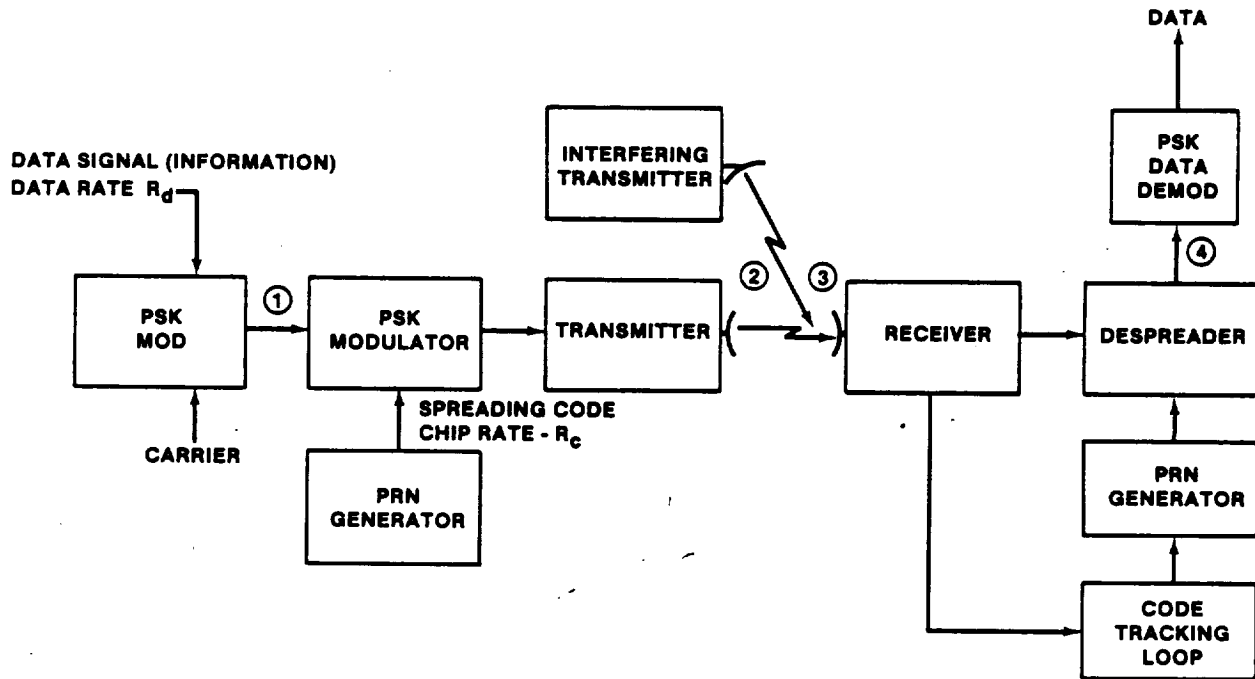
FIGURE 8.- SPREAD SPECTRUM SYSTEM CONFIGURATION.

As noted earlier, the Orbiter despreader design is unique because of several factors associated with the TDRSS forward communication channel. To meet the CCIR flux-density requirements, the forward link rf signal is spread using a PN sequence with chip rate R = 11.232 Mbps and the sequence length N = 2047 bits. The information transmitted over the TDRSS forward link to the Orbiter can be either 32 kbps or 72 kbps of data, rate one-third, convolutionally encoded. Since the despreader must operate for either rate, the worst case condition is encountered for the 72-kbps mode. For this case, the effective despreader information rate is the channel encoded symbol rate of 216 kbps. Thus, the ratio of chip rate to information rate is

$$\frac{R_c}{R_d} = \frac{11.232 \times 10^6}{216 \times 10^3} = 52 \tag{4}$$

This ratio is considerably lower than normally encountered in spread spectrum systems; as a result, several potential system design problems exist. The TDRSS forward link transmitted power is 46.5 decibels (referenced to 1 watt), which results in a nominal carrier-to-noise spectral density (C/N_0) at the Orbiter despreader of 54 decibel-hertz. Since the system must operate with a Manchester data format and allow for Doppler frequency offsets and hardware frequency uncertainties, the despreader bandwidth must be on the order of 500 kilohertz. Thus, the nominal despread signal-to-noise ratio P_s/N, assuming 3 decibels correlation and filter losses, is approximately -7.0 decibels under nominal conditions during acquisition. With the condition just described, a critical signal detection problem exists for reliably acquiring and tracking the spreading code.

Figure 10 is a simplified block diagram of the Orbiter despreading system. The spread signal is filtered in a band-pass filter (BPF) with 3-decibel bandwidth of approximately 20 megahertz. The filtered spread signal is then coupled to three product detectors (multipliers), where it is multiplied by a local replica of the PN spreading code. The process involved in acquiring code synchronization is now discussed. The local PN code is periodically stepped in phase by one-half of a chip width at a rate sufficiently slow to allow integration of the signal plus noise for detection purposes, but sufficiently rapid to ensure that maximum Doppler offset does not reduce the effective search rate by an unreasonable amount. When a phase is found at which the integrated signal plus noise reaches a value greater than the predetermined threshold setting, then phase synchronization is assumed, and the code stepping signal is removed. If the phase is truly correct, then the code tracking loop automatically pulls in, and code tracking is established.

731
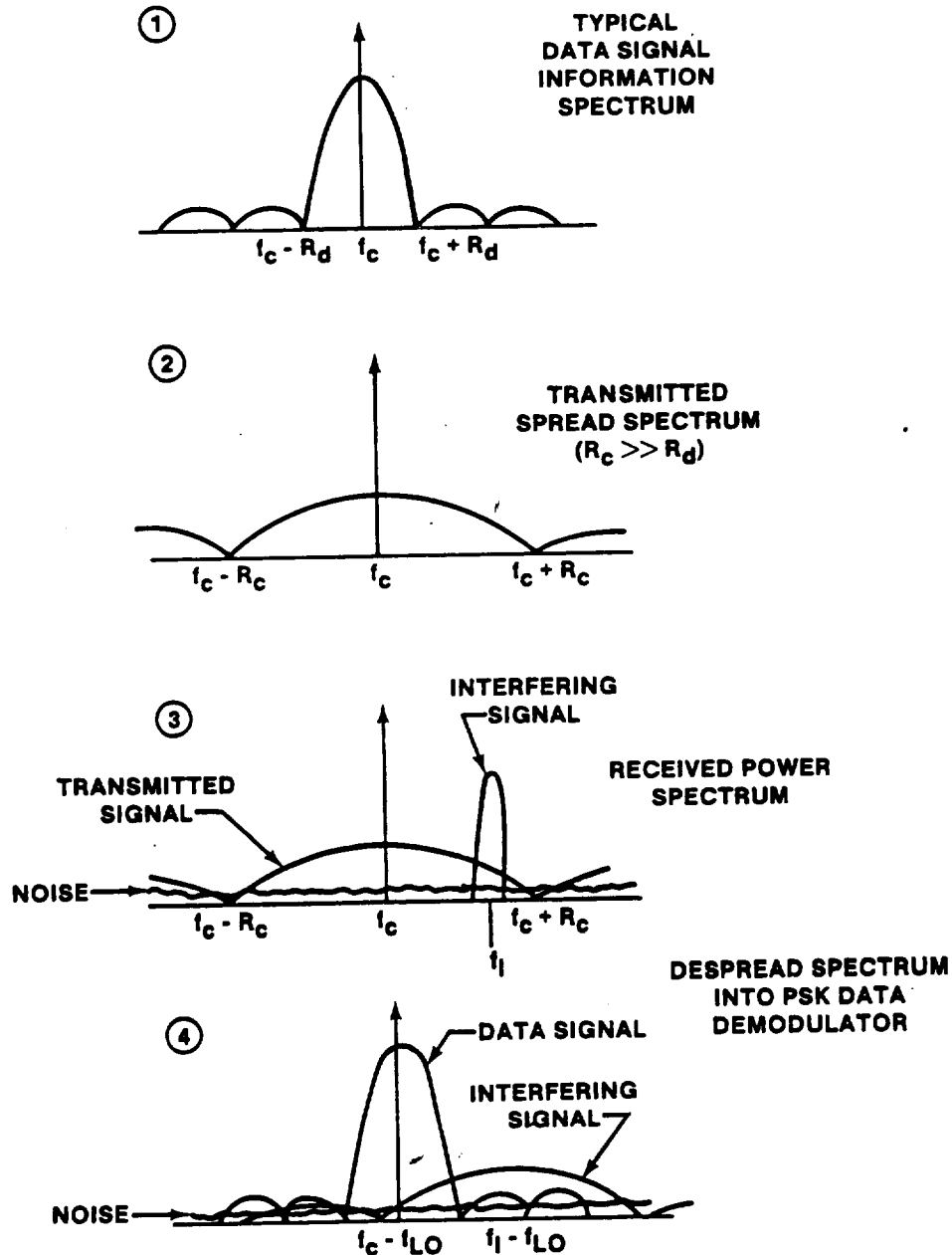
FIGURE 9.- SPREAD SPECTRUM TRANSMISSION.

Although the basic operation seems simple enough, several problems were encountered. A unique mechanization approach was necessary for updating the threshold setting in the lock decision process to ensure that drifts in channel gain and/or noise characteristics did not significantly affect the detection statistic. It is important to note that the same decision channel is used for signal detection and threshold updating. The threshold level is updated periodically, even when the system is tracking, by offsetting the PN code to the acquisition channel multiplier and thereby creating an uncorrelated condition and allowing the detector to sample system noise for threshold adjustment. This process is required to remove variations in system noise level due to channel gain variations and is referred to as an adaptive threshold.

Because of the low SNR's and the Doppler frequency offsets, the design of the code tracking loop required two loop bandwidths: a wideband acquisition loop and a narrow tracking loop. To ensure that
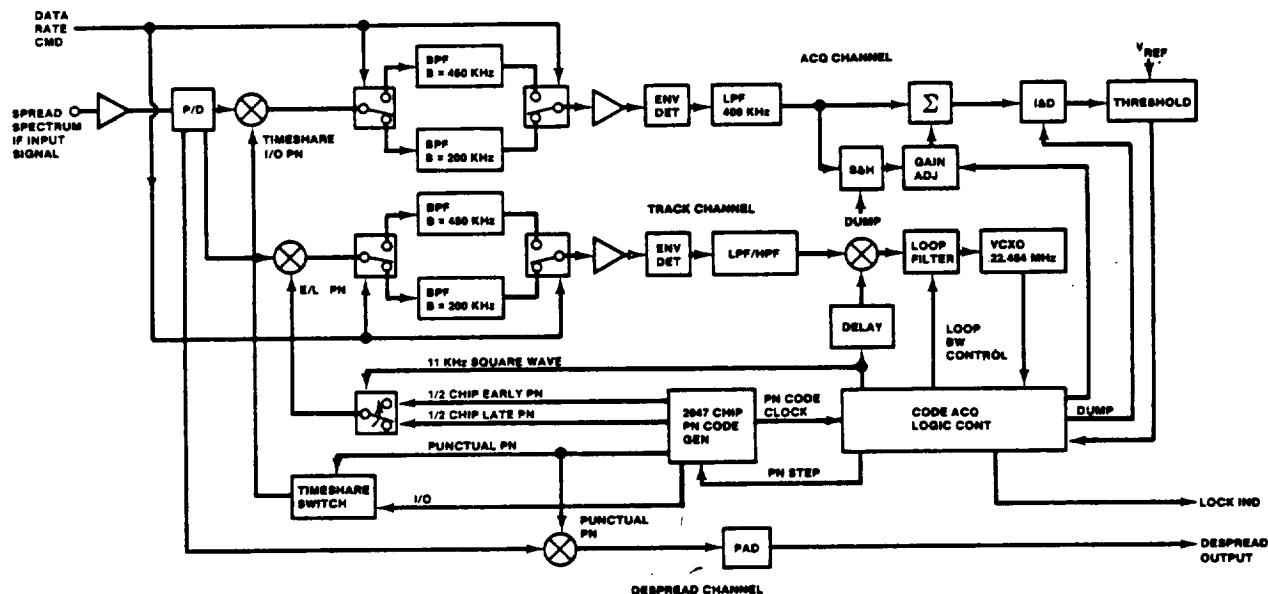
FIGURE 10.- S-BAND SPREAD SPECTRUM PROCESSOR (SSP) FUNCTIONAL DIAGRAM.

the loop will remain in lock sufficiently long after acquisition occurs, it is required that the loop bandwidth be reduced after tracking has been achieved. Care must be exercised in the bandwidth reduction to ensure that the switching transient does not cause the loop to unlock. A time delay before the loop bandwidth was switched and a stepped reduction in bandwidth was necessary to accomplish the desired results.

Of primary importance is the strategy employed in the process of acquiring code synchronization. Because of the low signal-to-noise condition and the desire for rapid acquisition, a strategy is needed by which synchronization can be achieved as quickly as possible, but with a high degree of confidence that the lock state is reached only when a valid synchronization condition is detected, and by which lock will be maintained for a significant length of time (90 minutes). To accomplish this, a serial search lock strategy is employed. The acquisition algorithm is illustrated by the flow diagram in figure 11 (ref. 7). The process followed is outlined in the following paragraphs.

Search is initiated and each phase position (cell) of the code is tested for some period of time T, which is selected to provide sufficient integration for a high probability of detection but small enough to allow rapid dismissal and to ensure that Doppler offset does not significantly increase the search time. Once a cell in which the integrated signal-plus-noise level exceeds the preset threshold is reached, a hit is declared. The system advances to the lock state, and the code tracking loop parameters discussed previously are switched. Once the system is in lock, five consecutive misses are required to cause loss of lock and reinitiation of the search process. Some of the significant features and critical parameters which are required in such a search/lock strategy are as follows.

1. The search mode threshold setting should be such that the probability of false alarm is in the vicinity of 10^{-2}. Lower probabilities of false alarm (10^{-6}) will result in extremely rapid degradation (increase) in acquisition time as the SNR decreases.

2. In lock, the probability of false alarm can be low since the desire here is to ensure that the system remains locked and, thus, a high probability of detection is necessary. The lock mode employs reset counters to reduce the probability of false dismissal to a sufficiently low value. A mean time to unlock on the order of 5400 seconds at a C/N_0 of 54 decibel-hertz is required for the Shuttle.

The theoretical mean acquisition time as a function of carrier-to-noise density and code Doppler offset in chips per second, for the Shuttle acquisition algorithm, is shown in figure 12.

For the Shuttle TDRS link, the forward link channel performance degradation in bit error probability (BEP) was specified to be less than 1.0 decibel. Test results obtained at the JSC ESTL verified that this specification was met. Tests also indicated that at strong C/N_0 values (65 decibel-hertz), the code tracking loop would false lock. Prior to the C/N_0 at which a solid false

733
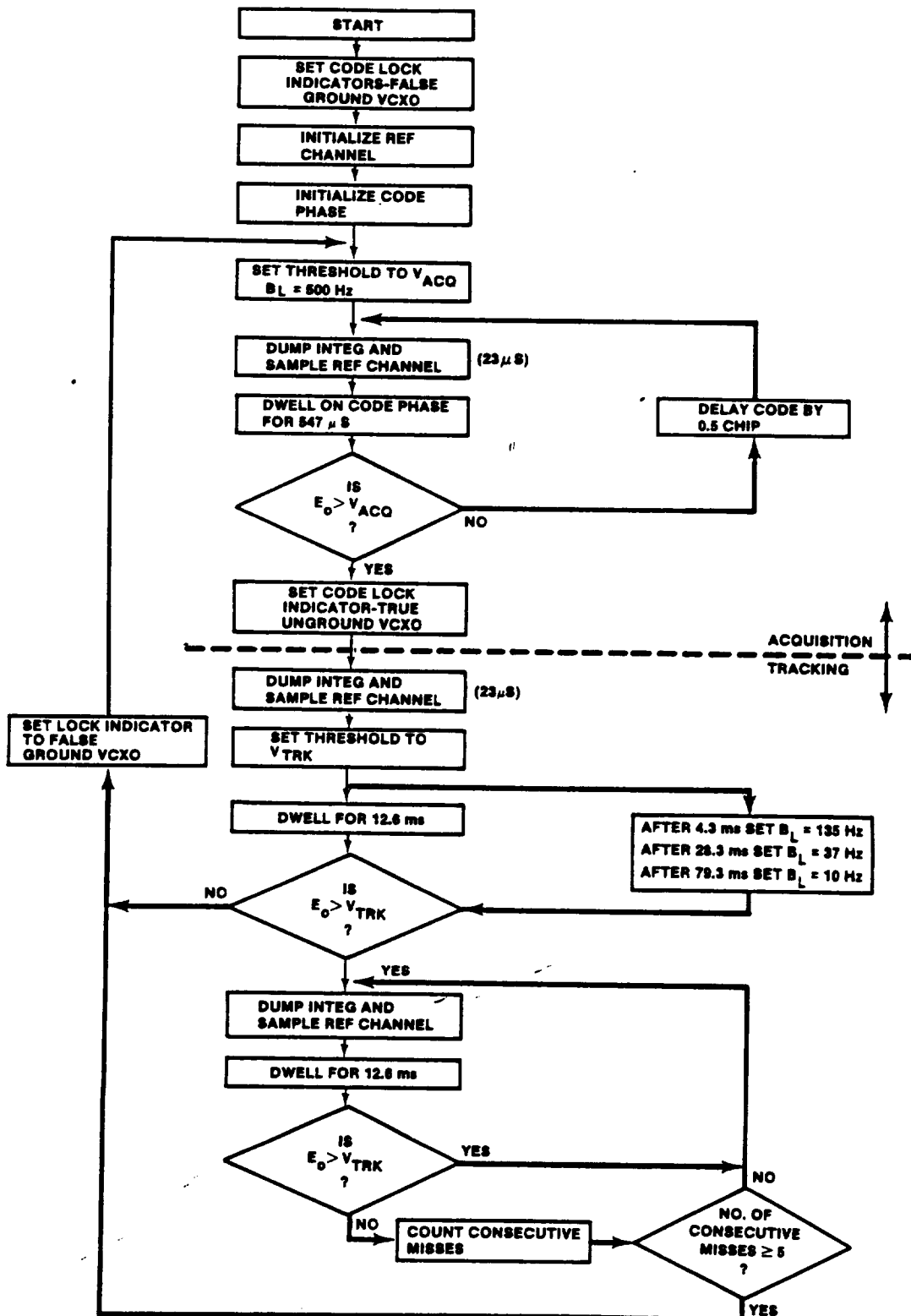
FIGURE 11.- SSP ACQUISITION-TRACKING ALGORITHM (S-BAND).

734
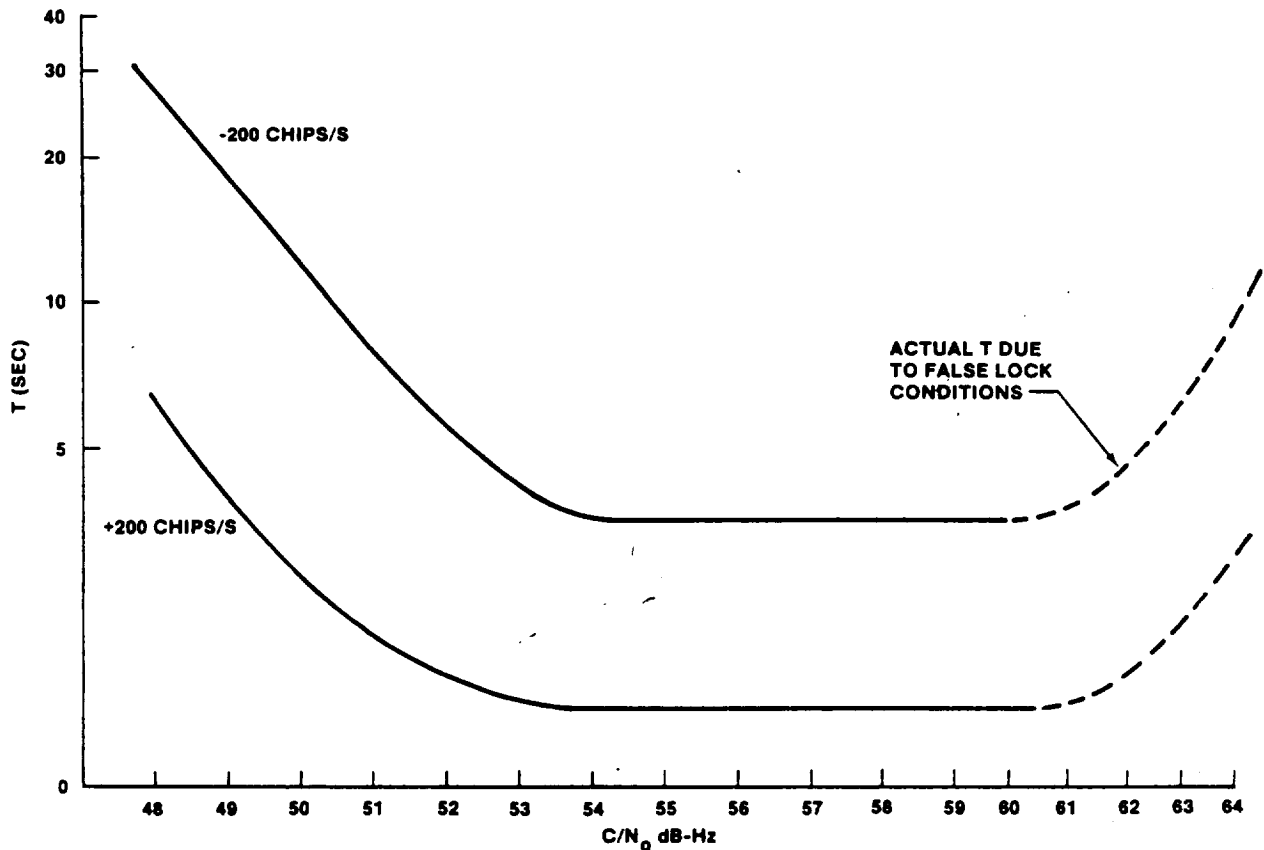
FIGURE 12.- S-BAND MEAN ACQUISITION TIME THEORY (WITH CODE DOPPLER OFFSET), LOW DATA RATE.

lock occurs, an increase in acquisition time is seen. This effect is illustrated by the dashed portion of the curves in figure 12, and is attributed to filtering effects giving rise to partial correlation outside the desired lock region. Figure 13 illustrates the unwanted correlation effects of a Tchebycheff band-pass filter on a typical Tau dither loop error signal (ref. 8).

ANTENNA GAIN/COVERAGE

Four quad antennas are used for the TDRS S-band communications. These antennas are located approximately 90° apart in the Orbiter roll plane and conform to the Shuttle inner moldline (fig. 14), which is the contour of its aluminum skin. The multiple-layer thermal protection system (TPS) is installed over the antennas.

Each of the four quad antennas has two beam positions, providing eight total beams around the Shuttle. These two beam positions are required to cover an angular sector of 140° in the pitch plane by 100° in the roll plane. This sector coverage is required to produce the specified gain coverage of 4 decibels over 85 percent of the sphere.

The quad antenna is a two-element array, which is oriented in the Shuttle nose-to-tail direction. The two elements are fed in quadrature, and their excitations are interchanged by an electromechanical transfer switch. The element itself is a crossed dipole in a square cavity, which provides circular polarization.

A typical measured composite coverage is shown in figure 15 for the 2041.9-megahertz frequency. This coverage is 63 percent at the 4-decibel gain level and is substantially less than the specified 85 percent. The coverage difference between theoretical and measured corresponds to a gain difference of approximately 0.5 to 1.0 decibel depending on the S-band operational frequency. This difference may be a result of the TPS effects and loss variations in stripline, switch, and cable components (ref. 9). The initial specified coverage of 85 percent at the 4-decibel level has been relaxed to an average value of 50 percent for the four operational S-band frequencies.

735
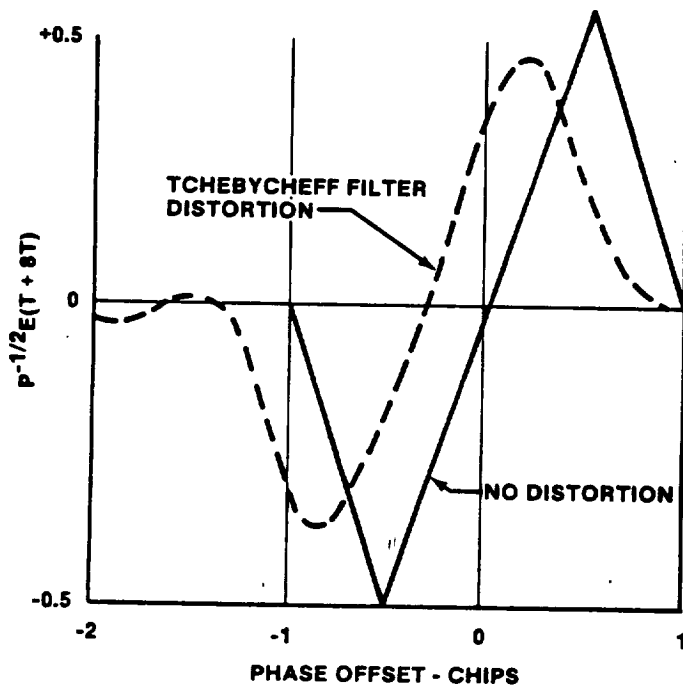
FIGURE 13.- EFFECT OF TCHEBYCHEFF BAND-PASS
FILTER ON A TYPICAL TAU DITHER LOOP ERROR
SIGNAL.
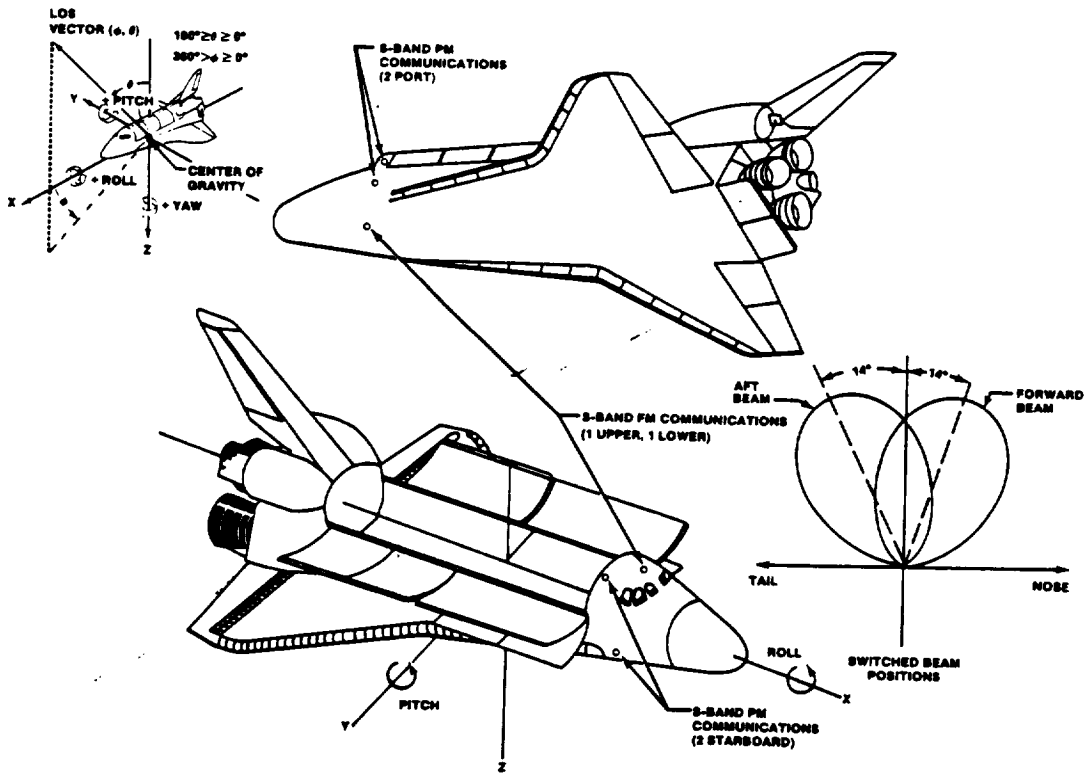
FIGURE 14.- SHUTTLE S-BAND ANTENNA LOCATIONS.

SWITCHED BEAM ANTENNAS
FREQUENCY = 2041.9 MHZ
THETA INCREMENT = 2 DEG
PHI INCREMENT = 2 DEG


GAIN CODES

□   ▪   ▪
0<G<2   2<G<4   G>4DB
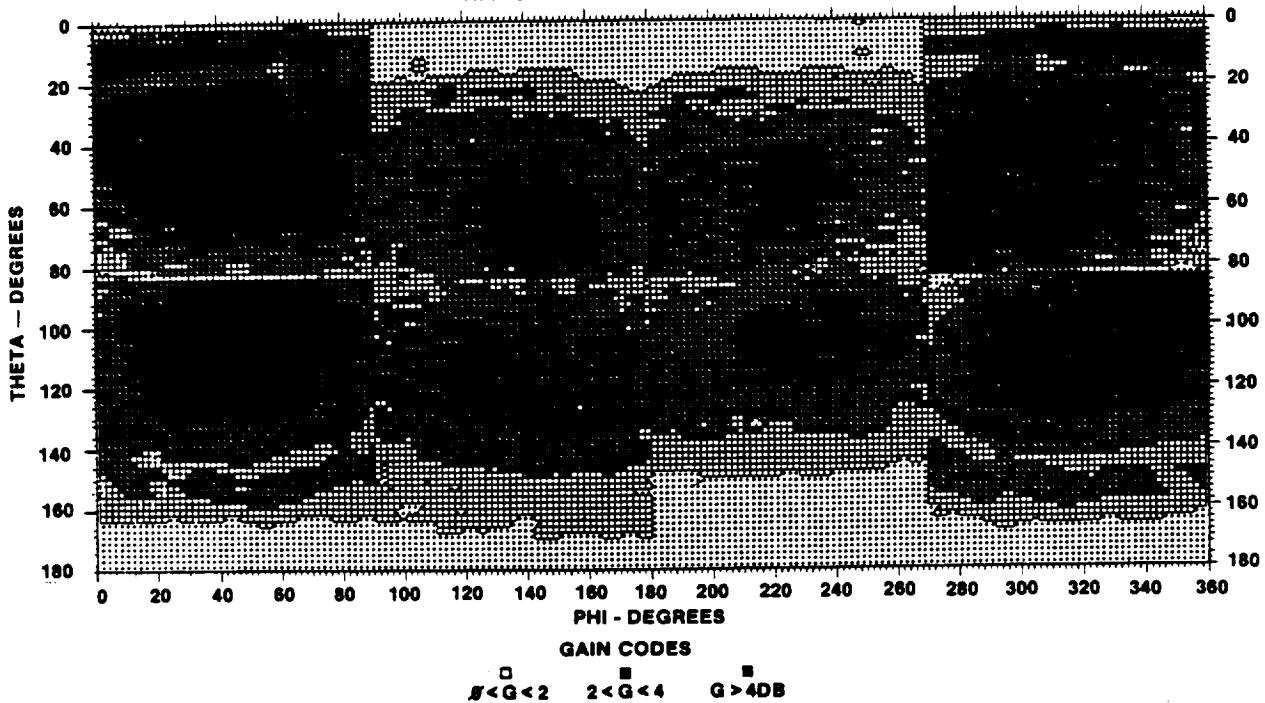
FIGURE 15.- MEASURED S-BAND QUAD ANTENNA SYSTEM COMPOSITE COVERAGE.

Since the desired gain/coverage capability has not been achieved with the existing TDRS switched-beam quad antenna system, some limited phased-array antenna development is continuing. A software simulation has been developed to analyze potential spherical coverage capability as a function of the number of beams formed by the switching array. Figure 16 illustrates the simulation results of gain over 85 percent of the sphere compared to the number of beams. Breadboard arrays are being evaluated at JSC for potential future applications on the Shuttle.

GSTDN AND AF/SCF COMMUNICATION MODE TECHNIQUES

One of the key areas of concern for the direct Shuttle to Earth communications system was the desire for rapid and automatic signal acquisition of the PM frequency links. Since an all-digital link design was dictated by TDRS and other operational considerations, a PSK modulation technique should allow acquisition with data modulation present on the carrier signal. However, navigational requirements established the need for a ranging function on the S-band communications channel. This requirement resulted in addition of a subcarrier to the uplinks and downlinks which carried the ranging signals of the GSTDN tone ranging system. The subcarrier was phase modulated by the ranging tones, and both the data and the subcarrier phase modulated the uplink and downlink S-band carriers. The net result of this ranging function addition was that PSK modulation could no longer be used for the GSTDN links. The ground station receiver was not capable of receiving a PSK signal; therefore, the downlink design was residual carrier PM from conception.

The television and recorded data are transmitted over a wideband FM link to provide sufficient bandwidth for the video signal or to allow dump of recorded data simultaneously with transmission of operational data on the PM links. The GSTDN and AF/SCF downlink frequencies are identical; however, the uplinks differ in frequency. Thus, the network transponder design had to be capable of operating with two coherent turnaround ratios (one for NASA GSTDN and the other for the USAF AF/SCF). Also, since the range from the Shuttle to the Earth is much closer than the range from the Shuttle to TDRS, a low-power transmit mode and less sensitive receive mode was provided for the direct Earth PM links. Broad antenna patterns for nearly continuous coverage with a minimum of vehicle attitude constraints were required for the PM and FM antenna systems.
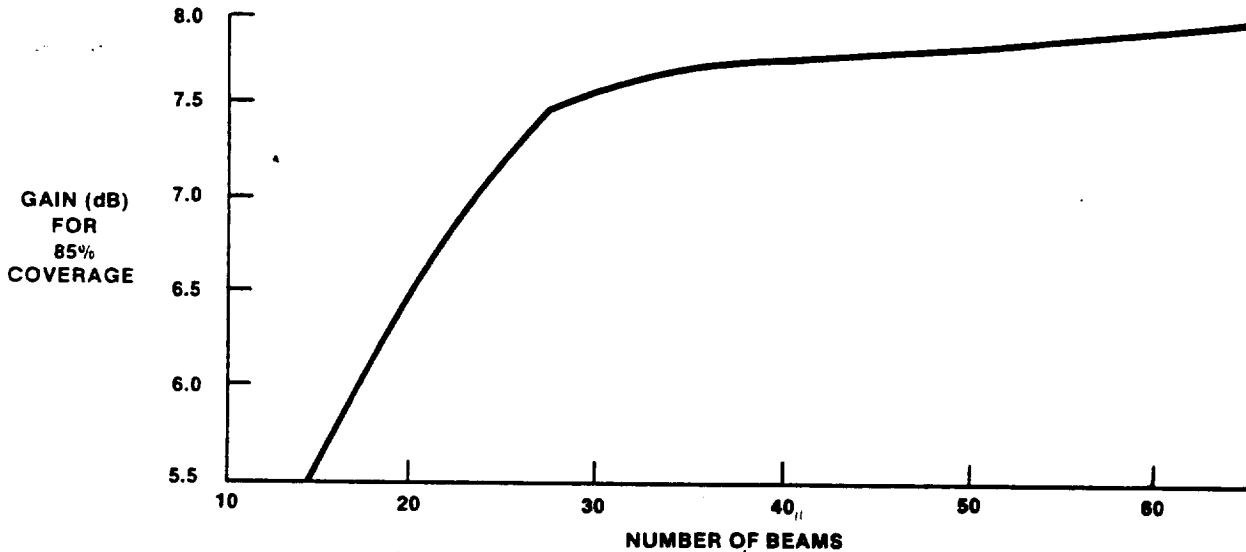
FIGURE 16.- SOFTWARE SIMULATION RESULTS OF GAIN FOR 85 PERCENT SPHERICAL COVERAGE WITH NUMBER OF BEAMS AS A VARIABLE.

RADIOFREQUENCY ACQUISITION AND CRITICAL PM MODULATION INDEX

As initially designed, the Shuttle S-band network receiver was to operate with a PSK uplink signal modulation format. Traditionally, a Costas loop is used in such receivers to reconstruct the totally suppressed carrier. However, for the Shuttle S-band uplink when ranging and data are both present, the Costas loop must acquire and track a residual (PM) carrier. As a result, several questions arise relative to the Costas loop performance under these conditions. It was also found that automatic acquisition could not be achieved even when PSK modulation was present because of the distortion effects of the Costas loop arm filters (ref. 10). These effects created stable false-lock points at frequencies related to the data rate and submultiples of the data rate as a result of data format repetitions, such as synchronization words and multiplexed voice words which contain alternate ones and zeros a vast majority of the time (when no speech is present). False locks become prevalent for some modes at carrier-to-noise density ratios as low as 58 decibel-hertz, which is only 4 decibels greater than expected levels for TDRS operations.

The rf acquisition problem is illustrated in figure 17, which shows the primary false-lock components associated with the uplink GSTDN mode using the high-rate data format. The TDM data rate in this case is 72 kbps; hence, a strong false-lock component results at the carrier frequency ±72 kilohertz. As seen in figure 17, false locks can also occur for carrier offsets of ±18 and ±54 kilohertz as a result of the multiplexed voice channel idle patterns (alternate ones and zeros), and at ±36 kilohertz as a result of the basic TDM format.

If voice is present, the ±18- and ±54-kilohertz lock points disappear because of the randomizing of the voice multiplexed word patterns. This fact, together with the introduction of rate one-third coding to increase the basic channel symbol rate to 216 kbps, was effectively employed to alleviate false-lock susceptibility for most of the launch trajectory (i.e., until Doppler shifts cause the one-half data-rate term to be within the receiver acquisition sweep range (ref. 11)). Figure 18 illustrates the uplink false-lock components of this special launch communication mode. To ensure that false-lock points do not exist within the carrier acquisition sweep range for a significant portion of launch communications coverage, two basic changes were made to the launch communication mode. First, a continuous low-level-noise modulation is introduced into the voice delta modulators. This continuous modulation in effect randomizes the voice word patterns and removes the associated false-lock components. Second, the data-rate multiplication due to encoding increases the channel symbol rate to 216 kbps; therefore, the one-half data-rate term now occurs at 108 kilohertz, which is beyond the acquisition sweep range of the Shuttle receiver with zero Doppler offset. As Doppler effects shift the received carrier frequency, a point is reached at which the 108-kilohertz term will fall within the acquisition sweep region. The time into launch at which this occurs is maximized by offsetting the launch-site transmitter frequency to compensate for Doppler effects as much as possible without causing the opposite 108-kilohertz component to appear within the sweep range.

The on-orbit acquisition process is normally accomplished without modulation applied to the up-

(ZERO DOPPLER, ±85 KHz ABOUT CARRIER)

72 Kbps TDM, 1-0 VOICE IDLE PATTERN, RANGING-ON

—— SIGNIFICANT FALSE LOCK
COMPONENTS FROM TDM
SIGNAL DATA RATE

— — SIGNIFICANT FALSE LOCK
COMPONENTS DUE TO VOICE
IDLE PATTERN

FREQUENCY (kHz)

-72   -54   -36   -18 f_c +18   +36   +54   +72

-85 KHz   +85 KHz

SSO RECEIVER SWEEP RANGE
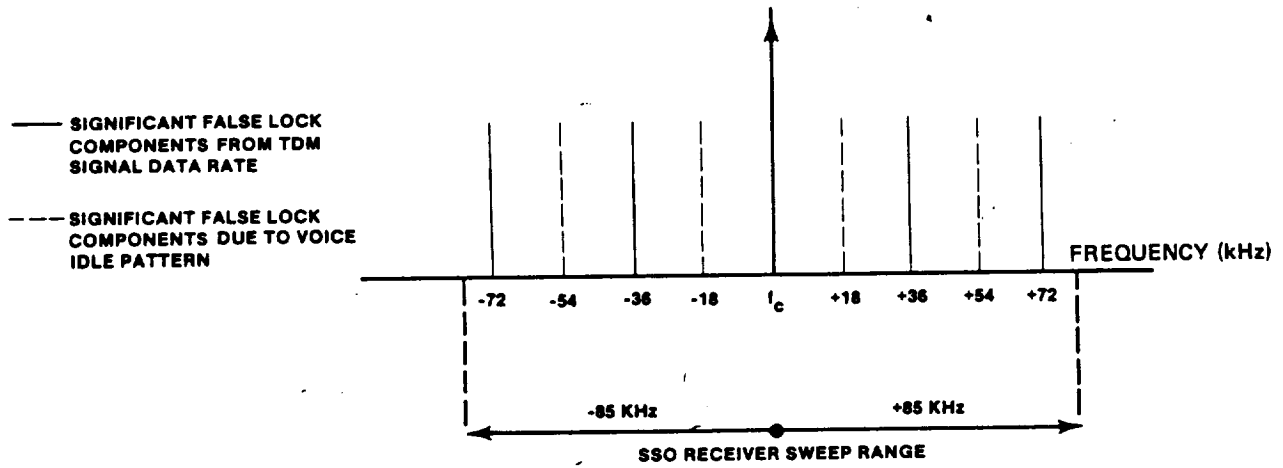
FIGURE 17.- GSTDN UPLINK SIGNAL FALSE-LOCK COMPONENTS.

(ZERO DOPPLER, ±108 KHz ABOUT CARRIER)

**216 Kbps CONVOL. ENCODED TDM, 1-0 VOICE IDLE PATTERN
RANGING-ON**

—— SIGNIFICANT FALSE LOCK
COMPONENTS FROM TDM
SIGNAL DATA RATE

— — SIGNIFICANT FALSE LOCK
COMPONENTS DUE TO VOICE
IDLE PATTERN

-108   -72   -54   -36   -18 f_c +18   +36   +54   +72   +108

-85 KHz   +85 KHz

SSO RECEIVER SWEEP RANGE

* ±18, ±36, ±54, ±72 KHz COMPONENTS NOT PRESENT
DURING ACQUISITION/REACQUISITION (NOISE MODULATION
APPLIED TO VOICE CHANNEL)
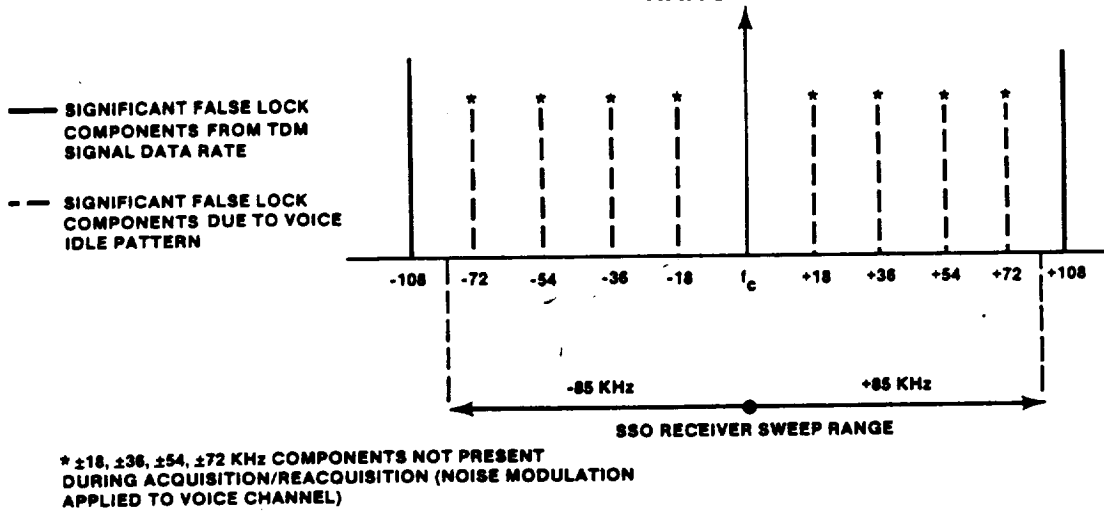
FIGURE 18.- UPLINK SIGNAL FALSE-LOCK COMPONENTS OF THE SPECIAL LAUNCH COMMUNICATION MODE.

link carrier for both direct (GSTDN) links and TDRS links. Since the ground receiver designs incorporate anti-sideband lock features, no significant false-lock problems were encountered by the GSTDN or TDRS ground station receivers.

In addition to the basic false-lock problems encountered with the Shuttle transponder, a phenomenon referred to as "critical modulation index" effect was encountered. Traditionally, a Costas loop is intended for use in receivers that must reconstruct a carrier reference from an input signal hav-

739

ing a completely suppressed carrier component (i.e., PSK modulation). However, for the Shuttle direct (GSTDN) uplink mode with ranging, the Orbiter transponder Costas loop is required to acquire and track a PM signal (i.e., when a residual carrier component is present in the signal spectrum), as is illustrated in figure 19. The means by which the ranging subcarrier is extracted using the in-phase modulation reference signal generated by the Costas loop is shown in the figure.

For the case of a Costas loop operating on a linear modulated signal with digital TDM data and a sine-wave ranging subcarrier, the error signal in the loop can be defined as follows.

If the input signal is given by equation (5)

$$s(t,\theta) = \sqrt{2A}\ \sin\left[\omega_0 t + \overbrace{\theta_1 d(t)}^{\text{TDM data}} + \overbrace{\theta_2 \sin(\omega_{sc} t + \beta R(t))}^{\text{Ranging subcarrier}}\right] \tag{5}$$

then the error signal in the loop $Z_0(t)$ can be shown to have the form of equation (6).

$$Z_0(t) = A J_0^2(\theta_2)\left[D\sin^2\theta_1 - \cos^2\theta_1\right]\sin\psi \tag{6}$$

where

ω_{sc} = ranging subcarrier radian frequency and $\omega_{sc} \gg$ than the low-pass arm filter 3-decibel bandwidth

D = filter distortion factor; $D = 1$ for infinite-bandwidth arm filters

θ_1 = TDM data PM modulation index (radians)
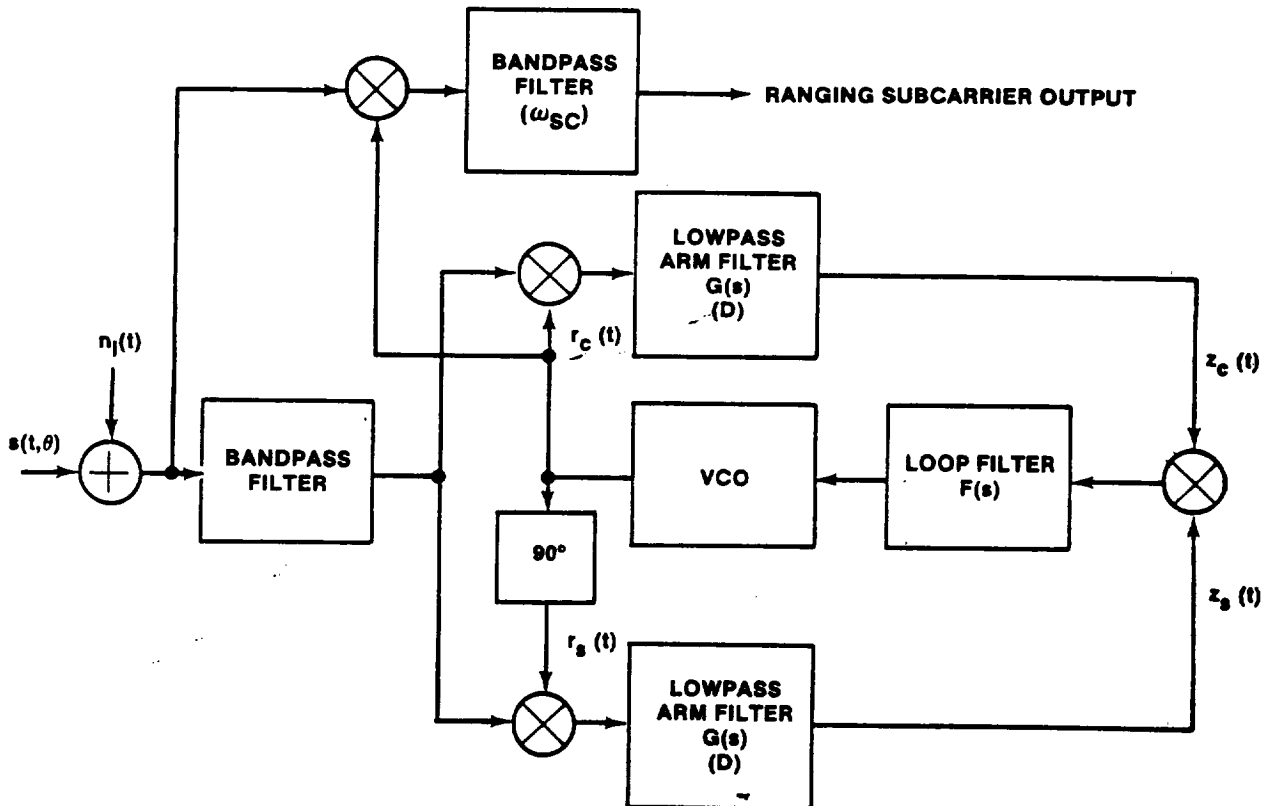
FIGURE 19.- COSTAS LOOP AND RANGING DEMODULATOR.

θ_2 = ranging subcarrier modulation index (radians)
β = ranging tone PM modulation index (radians)
$R(t)$ = ranging tone signals
J_0 = Bessel function of first kind and order zero
$A \sin \omega_0 t$ = carrier signal (unmodulated)

Note that the error signal $Z_0(t)$ disappears (i.e., goes to zero) for the following conditions.

1. $J_0^2(\theta_2) = 0$; when $\theta_2 = 2.4$ radians

2. $\theta_1 = \cot^{-1} \sqrt{D}$; when $\theta_1 = \pi/4$ radians or 45° and infinite bandwidth (i.e., $D = 1$) is assumed

For the Shuttle network transponder, the Costas loop filter distortion factors have been rigorously defined (ref. 12). The critical modulation index $(\theta_1)_{cr}$ for which the Shuttle Costas loop cannot acquire or track the GSTDN ranging modes for the various TDM data rates of interest is given in table 5.

It is obvious from equation (6) that as the filter distortion factor approaches unity, the signal power available for tracking (i.e., error signal) approaches that for the PSK channel. For PSK, the error signal would become

$$Z_0(t) = AD \sin 2\psi \quad (\text{since } \theta_2 = 0 \text{ and } \theta_1 = \pi/2 \text{ radians}) \tag{7}$$

The acquisition performance of the loop in the PM mode of operation will always be degraded over that for a PSK modulation mode. Table 6 illustrates the calculated and measured acquisition threshold for a representative Shuttle network transponder Costas loop in the PSK and PM (residual carrier) modes of operation.

TABLE 5.- CRITICAL MODULATION INDEX $(\theta_1)_{cr}$

TDM data rate	Costas loop arm filter, 3-dB bandwidth, kHz	Filter distortion factor (D)	$(\theta_1)_{cr}$, rad
32 kbps (Low data rate, uncoded)	147.5	0.886	0.8157
96 kbps (Low data rate, coded)	147.5	.6636	.8872
72 kbps (High data rate, uncoded)	147.5	.8884	.851
216 kbps (High data rate, coded)	147.5	.670	1.003

The performance of the ranging channel is also dependent on the selection of the TDM data modulation index. The ranging subcarrier is extracted by demodulating the input signal with an in-phase reference generated by the Costas loop. The signal power available to the ranging channel is given by

$$P_r = 2P \cos^2(\theta_1) J_1^2(\theta_2) \cos^2\psi \tag{8}$$

where

P_r = the power available in the ranging channel
θ_1 = the data PM mode index
θ_2 = the ranging subcarrier modulation index
β = the total received power level
ψ = the Costas loop dynamic phase error
J_1 = the first-order Bessel function of the first kind

741

TABLE 6.- ACQUISITION THRESHOLDS

Parameters			Threshold P_r/N_0, dB-Hz	
Data PM index, rad	Subcarrier PM index, rad	Arm filter bandwidth, kHz (a)	Calculated	Test (a)
PSK (216-kbps data)				
$\pi/2$	0	147.5	47.68	45.6
216-kbps data plus ranging				
1.25	1.0	147.5	55.84	56.1
1.1	1.0	147.5	61.15	61.6
1.125	1.0	147.5	59.66	60.6
1.375	1.0	147.5	54.26	53.8

[a]September 1980 ESTL test results.

As the data modulation index is increased above its critical value, the Costas loop tracks better. However, the factor $\cos \theta_1$ decreases and hence the ranging power is reduced. Obviously, a trade-off exists with respect to selection of θ_1. If the data modulation index falls below the critical value or if data are removed completely, the in-phase and quadrature demodulation reference signals switch roles and the ranging channel power P_r tends toward zero depending on the exact value of the loop phase error ψ. Thus, to extract ranging modulation, the data modulation must be present and at a modulation index above its critical value.

FREQUENCY MODULATION OPTIMUM FREQUENCY DEVIATIONS

For the Shuttle digital FM links, it was necessary to optimize the modulation parameters because of the relatively low transmitter power (10 watts) and the low antenna gains of the FM hemispherical coverage antennas. For a digital frequency-shift keying (FSK) system with coherent matched-filter detection and assuming "zero" correlation between transmitted symbols, the performance has been shown to be 3 decibels worse than for coherent PSK systems. For such a system, the probability of error is given by equation (9).

$$ Pe = \frac{1}{2} \, erfc \, \sqrt{\frac{(1 - \rho) \, E_b}{2N_0}} \tag{9} $$

where

E_b = the energy per bit time
N_0 = the receiver noise spectral density
erfc = the complementary error function

and ρ is the normalized symbol correlation coefficient given by equation (10).

$$ \rho = \frac{1}{E_b} \int_0^T S_1(t) \, S_2(t) dt \tag{10} $$

where $S_1(t)$ and $S_2(t)$ are the transmitted symbols. However, it is not necessary that there be zero correlation between transmitted symbols $S_1(t)$ and $S_2(t)$. For the case of continuous-phase (i.e., nonswitched) digital FM links, it can be shown that ρ can take on negative values. Equation (11) represents the value of ρ for a continuous-phase FM transmitter modulated with binary non-

742

return to zero (NRZ) symbols.

$$\rho = \frac{\sin\left[2\pi(2\Delta f)\ T_S\right]}{2\pi(2\Delta f)\ T_S}$$

(11)

where

Δf = the peak frequency deviation of the FM transmitter (hertz)
R = symbol data rate
T_S = NRZ symbol bit time

As seen from figure 20 for orthogonal performance (i.e., ρ = 0), the frequency deviation is Δf = 0.25R. However, for optimum "best" performance, ρ = -0.22 and the frequency deviation is Δf = 0.36R. Thus, performance of an optimum continuous-phase digital FM channel should be only 2.2 decibels worse than performance of an optimum PSK channel. This surprising result constitutes a performance bound on FSK systems using suboptimum detection schemes.

$$\rho = \frac{\text{Sin}\ 2\ \pi\ (2\Delta f)T_s}{2\ \pi\ (2\ \Delta f)\ T_s} \qquad T_s = \frac{1}{R}\ ;\ \text{WHERE R IS THE SYMBOL RATE}$$
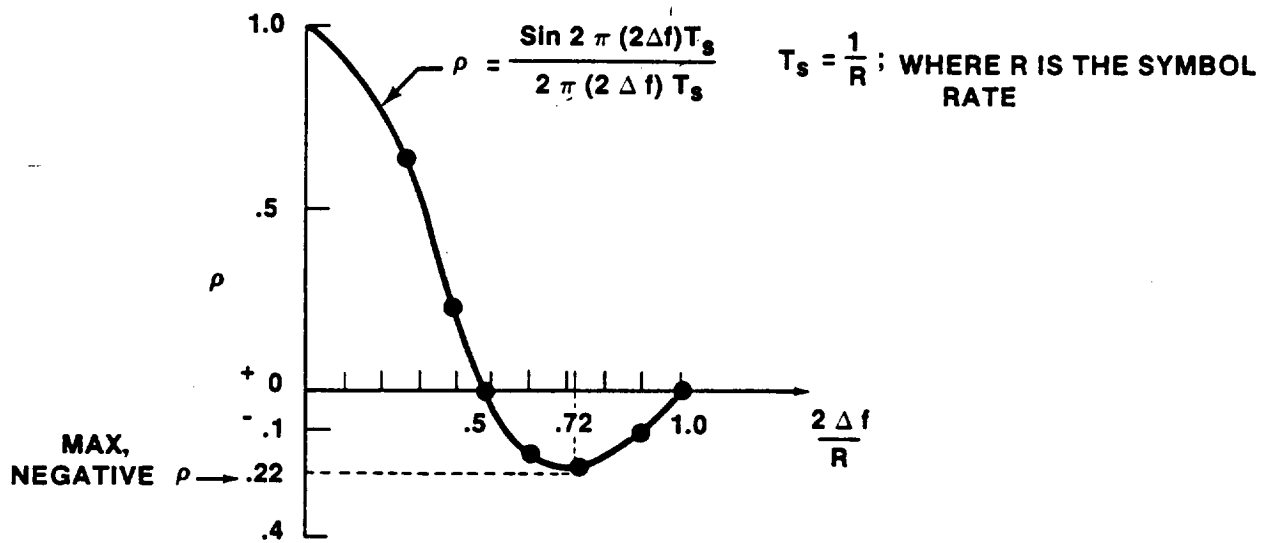
$$P_{E_O} = \frac{1}{2}\ \text{erfc}\sqrt{\frac{.5\ E_b}{N_o}} \rightarrow \text{ORTHOGONAL PERFORMANCE}\ \left[\rho = 0, \frac{2\ \Delta f}{R} = .5\right]$$

$$P_{E_B} = \frac{1}{2}\ \text{erfc}\sqrt{\frac{.61\ E_b}{N_o}} \longrightarrow \text{BEST PERFORMANCE}\ \left[\rho = -.22, \frac{2\ \Delta f}{R} = .72\right]$$

$$\therefore P_{E_B} \longrightarrow \text{REPRESENTS PERFORMANCE BOUND ON COHERENT FSK 2.2 dB WORSE THAN COHERENT PSK}$$

FIGURE 20.- ρ VERSUS FREQUENCY DEVIATION FOR CONTINUOUS-PHASE FM DIGITAL MODULATION.

In the Shuttle case, the FM link was designed for the optimum Δf at the highest channel digital data rate of 1024 kbps. Another parameter which affects the optimum performance of the linear FM digital channel is the ratio of i.f. filter bandwidth to the data rate. Table 7 shows the values of normalized optimum Δf and ratios of i.f. filter bandwidth to data rate B/R for NRZ and biphase data formats (ref. 13).

Experimental results of Shuttle link performance using a linear FM discriminator followed by an integrate-and-dump bit synchronizer (fig. 21) agreed quite well with the theoretical performance for NRZ data. Figures 22 and 23 illustrate the experimental results obtained during tests at the JSC

743

TABLE 7.- OPTIMUM PARAMETERS FOR FM DIGITAL LINK

Data format	$\Delta f/R$	B/R
NRZ	0.360	1.4
Biphase[a]	.62	2.7

[a]Biphase optimum Δf was determined experimentally.

$\bullet_{1N}(t) \longrightarrow$ BAND-PASS FILTER AT $\left[\dfrac{\omega_{c_2} - \omega_{c_1}}{2}\right]$ $\longrightarrow$ LIMITER/DISCRIMINATOR $\longrightarrow$ BIT SYNCHRONIZER $\quad$ $\bullet_0(t)$ $\quad$ +1 $\quad$ -1

FIGURE 21.- SHUTTLE DIGITAL FM LINK DETECTION PROCESS.

RELATIVE E_b/N_0 REQUIRED TO MAINTAIN
$P_E = 10^{-4}$ IN (dB)

B/R = RATIO OF IF 3dB BANDWIDTH TO DATA RATE

$\Delta f/R$ = RATIO OF PEAK FREQUENCY DEVIATION TO DATA RATE

$\dfrac{B}{R} = .9$

$\dfrac{B}{R} = 5.0$

$\dfrac{B}{R} = 1.4$

$2\Delta f/R$
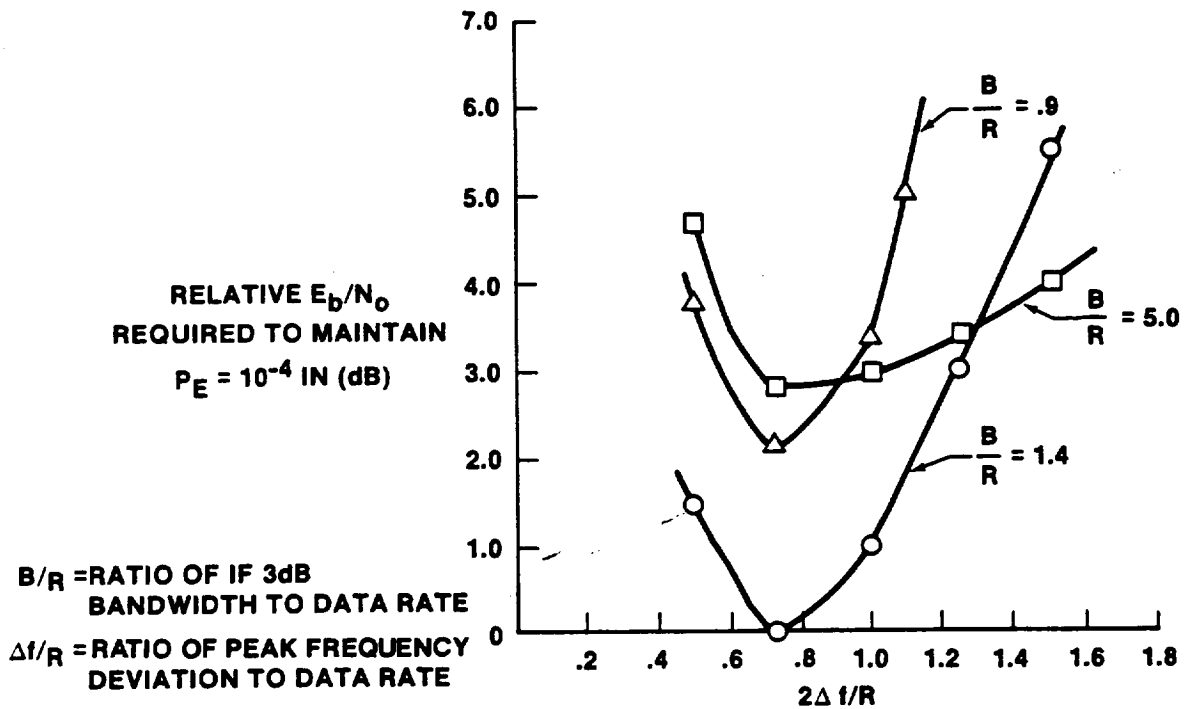
FIGURE 22.- RELATIVE BIT ERROR PERFORMANCE (NRZ DATA): DISCRIMINATOR DETECTION OF CONTINUOUS-PHASE FM MODULATION.

ESTL (ref. 13). Performance in terms of the relative E_b/N_0 required to maintain a 1×10^{-4} BER is shown as a function of frequency deviation Δf and receiver 3-decibel bandwidth B to digital data rate R ratio B/R. The optimum case tested is for B/R = 1.4 and a Δf of 0.36R as seen from figure 22 for NRZ digital data, and B/R = 2.7 and Δf = 0.65 for biphase digital data as seen from figure 23.
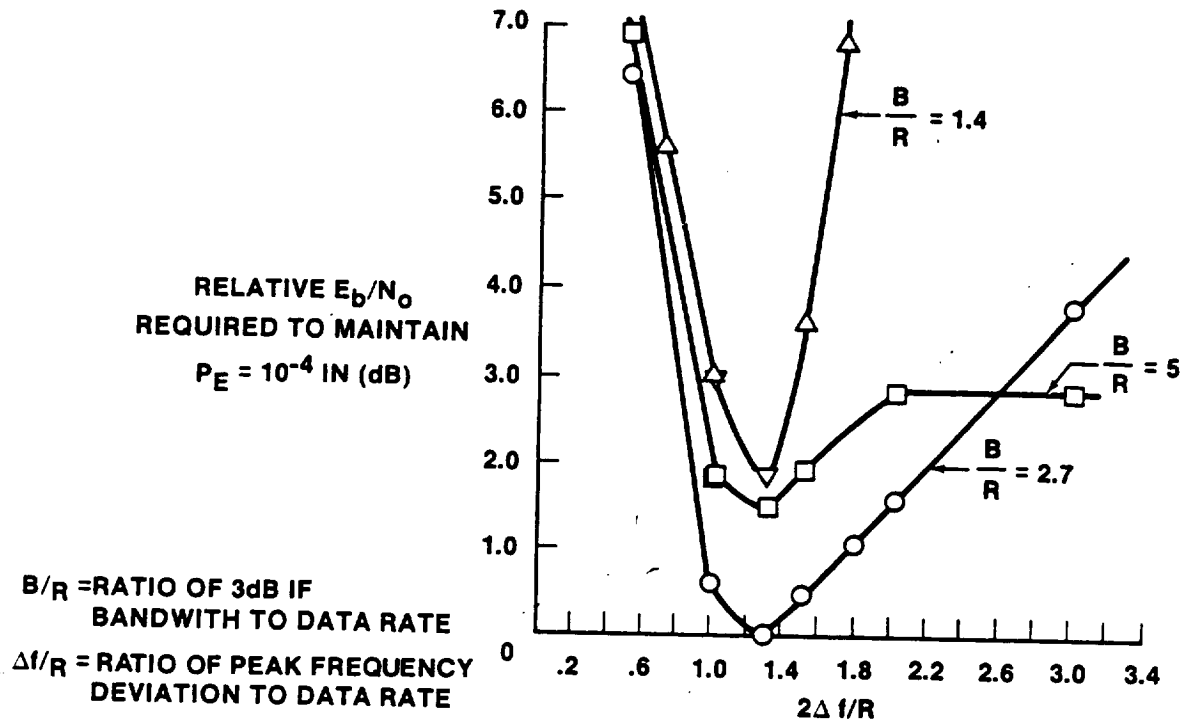
FIGURE 23.- RELATIVE BIT ERROR PERFORMANCE (BIPHASE DATA): DISCRIMINATOR DETECTION OF CONTINUOUS-PHASE FM MODULATION.

RANGING CHANNEL (SUBCARRIER MODULATION)

General Description

The ranging channel is used primarily during ascent and entry to provide a precision analog measurement of slant range between a GSTDN ground station and the Orbiter. The ranging signal consists of a combination of tones which are generated by the GSTDN ground station. This analog signal phase modulates a 1.7-megahertz subcarrier, which is then frequency-division multiplexed (FDM) with a baseband digital signal (32, 72, 96, or 216 kbps biphase-level format operational data). The resulting FDM signal then phase modulates the uplink carrier frequency. In the Orbiter receiver, a phase demodulator recovers the FDM signal; the 1.7-megahertz tone-modulated subcarrier is separated from the FDM signal by a BPF and amplified by an automatic gain control (AGC) circuit. This filtered, amplified ranging subcarrier is then FDM with a downlink baseband digital signal (96, 192, 288, or 576 kbps biphase-level format operational data). The resulting FDM signal phase modulates the downlink carrier frequency (which is coherent with the uplink carrier frequency). At the GSTDN station, a phase demodulator recovers the 1.7-megahertz tone-modulated subcarrier, which is then demodulated by a subcarrier phase demodulator. The recovered range tones are routed to a processor, in which slant range is determined.

Range Measurement

The range measurement data are instantaneous values of the total phase delay of a major tone from the time of transmission of the tone from the GSTDN station to the Shuttle to the time of reception of the tone back at the GSTDN station. The round-trip phase delay is provided in nanoseconds with a 1-nanosecond resolution. Each phase-delay measurement has a time tag; the measurement corresponds to the phase delay at a time within ±50 nanoseconds of the associated time tag. Each measurement is independent of previous measurements and is unambiguous to a range of 15 000 kilometers, with maximum 3σ range measurement errors of 10 meters noise and 20 meters bias.

The major tone currently used is 500 kilohertz. To resolve the total phase delay through the rf communications system, a series of lower frequency tones must be simultaneously transmitted through the system during initial acquisition. After an initial measurement of the total phase delay has been made, the transmission of low-frequency tones is discontinued until a loss of lock occurs and a

745

reacquisition is required. The modulation steps in obtaining the initial total phase-delay measurement are listed in table 8. The 500-kilohertz tone is modulated on the 1.7-megahertz subcarrier and transmitted to the Orbiter in step 1. When the return 500-kilohertz tone has been received on the

TABLE 8.- RANGING MODULATION SEQUENCE

Sequence step	Tones phase modulated on 1.7-MHz subcarrier	Remarks
1	500-kHz major tone	
2	500-kHz major tone 100-kHz minor tone	
3	500-kHz major tone 20-kHz minor tone	
4	500-kHz major tone 4-kHz minor tone	The 4-kHz minor tone is modulated by an 800-Hz tone using upper single sideband suppressed carrier (USSBSC) modulation with the lower sideband filtered so that it is 20 dB down.
6	500-kHz major tone 4-kHz minor tone	The 4-kHz minor tone is modulated by a 160-Hz tone using double sideband suppressed carrier (DSBSC) modulation.
7	500-kHz major tone 4-kHz minor tone	The 4-kHz minor tone is modulated by a 40-Hz tone using DSBSC modulation.
8	500-kHz major tone 4-kHz minor tone	The 4-kHz minor tone is modulated by a 10-Hz tone using DSBSC modulation.
9	500-kHz major tone	

ground and phase lock to the 500-kilohertz tone has occurred, the ranging equipment automatically changes to step 2 by adding a 100-kilohertz tone to the uplink. The equipment automatically proceeds through the remaining steps until only the 500-kilohertz tone remains. At this point, the first total phase-delay measurement is completed. Subsequent measurements can be provided at selected rates as high as 10 per second.

S-BAND NETWORK COMMUNICATION SUBSYSTEM

The S-band network equipment consists of 10 line replaceable units (LRU's) and associated antennas as shown in figure 24. The subsystem is redundant with the exception of the rf contacts in the antenna switch, the diplexers in the preamplifier, and the antennas with their associated rf cables. The general redundancy approach is to use the equipment in strings and avoid cross-strapped operations. A minimal amount of status information such as temperatures, AGC values, and rf power outputs is provided by the LRU's for relay in either real-time or delayed (recorded) telemetry.

The hardware is environmentally sealed and cold-plate cooled. The environmental design requirements were based on the controlled areas of the Shuttle equipment bays, and the equipment cannot withstand exposure to space environments. All S-band LRU's operate from 28-volt dc buses, and each LRU has the capability to operate from either of two redundant buses. The power distribution is carefully designed to maintain the string-redundancy approach. Internal LRU redundancy is maintained by physical separation and by including structural elements to provide isolation and prevent propagation of failures. See table 9 for LRU physical information.
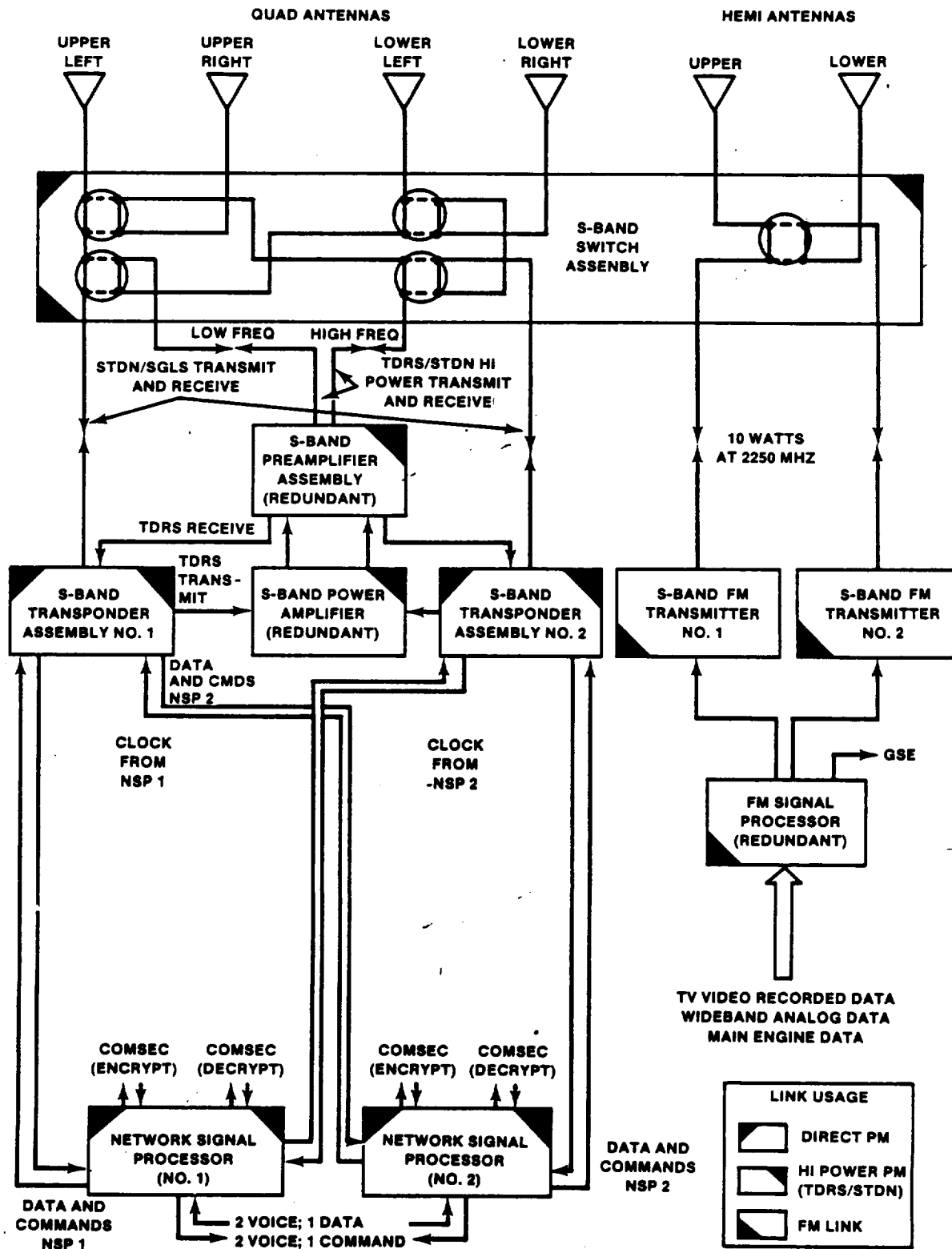
FIGURE 24.- S-BAND NETWORK COMMUNICATION EQUIPMENT.

TABLE 9.- S-BAND LRU PHYSICAL CHARACTERISTICS

LRU	Weight, lb	Approximate volume, in^3	Power, W
Network transponder (2 required)	35.8	1120	65 STDN/SGLS 48 STDN-Hi/TDRS
Preamplifier	25.6	790	35 Turn-on 25 After 10 min
Power amplifier	32.5	850	415 Operate 20 Standby
Switch assembly	7.7	335	2 Steady state 150 Switching
FM transmitter (2 required)	6.8	115	120
FM signal processor	12	395	9
Network signal processor (2 required)	18	720	30

As indicated in figure 24, the S-band network equipment is functionally divided into the PM and FM systems. The only common LRU is the antenna switch assembly, which provides similar but separate rf signal routing services for both systems. In the Shuttle operational era, the FM system will be a "kittable" (optional) flight item since it provides services on direct links only. The PM equipment provides four basic modes of operation, two of which are "low power" (SGLS and GSTDN) direct links and two, "high power." One high-power mode is a direct link (GSTDN-Hi Pwr) and the other is the satellite relay link (TDRS). In all cases, system control signals for operational modes are routed through the Ground Communications Interface Logic (GCIL) and configuration control is exercised by forward link commands. In contingencies, these controls can be exercised by onboard panel switches or keyboard entries to the onboard general-purpose computers (GPC's).

The heart of the S-band PM system is the network transponder (fig. 25). In all primary modes, it supports full duplex operation and is also capable of receive-only service. The LRU operates in a phase-coherent mode with a specified turnaround ratio and has the capability to turn around ranging data. The double conversion receiver employs a Costas detector. A spread spectrum processor is activated in the TDRS mode. The baseband and control module chooses various parameters in accordance with mode selection and controls the acquisition scenarios. In the low-power modes, all the transmitter power amplifier stages are active and the rf output is 5 watts. When a high-power mode is selected, the final stages are inactive to provide a lower (1 watt) level to drive the S-band power amplifier.

The S-band preamplifier supplies the diplex function in the high-power modes and also provides low-noise preamplification for the network transponder receiver. The preamplification is provided by uncooled parametric amplifiers followed by transistor amplifiers. The diplex function is not redundant. There are two diplexers; one is used for the high STDN frequency pair and the other, for the low STDN frequency pair. Internal switching allows the use of either preamplifier with either transponder and either power amplifier.

The S-band power amplifier is used in the high-power modes to amplify the output of the transponder. The LRU consists of two TWT's with their associated power converters and control circuits. The input portion of the LRU incorporates an rf switch to route either transponder output to either of the internal amplifiers. The LRU incorporates several protective devices for the TWT's. Each output is protected from mismatch damage by a circulator and load. The tubes are further protected from po-
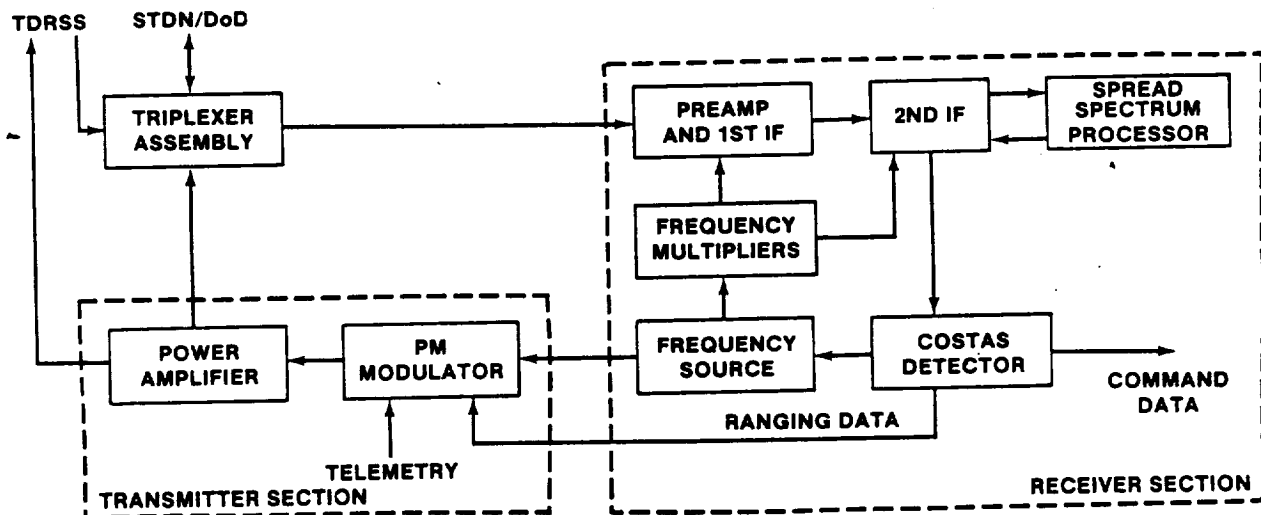
FIGURE 25.- NETWORK TRANSPONDER FUNCTIONAL BLOCK DIAGRAM.

tential collector thermal shock damage by a circuit which senses the absence of rf drive and shuts down the power supply or the high voltage to the tube. The power amplifiers typically produce 120 to 140 watts of rf output power.

The S-band antenna switch is internally redundant except for the rf head assembly. The LRU provides four transfer switches for the PM signal routing and one switch for the FM system. The input logic and switch drives are fully redundant. Control signals originate with the GPC system in the automatic mode and with the Orbiter control panel in the manual mode. The LRU logic receives inputs that indicate the equipment in use and the mode of operation. The internal logic then recognizes commands to select a given antenna and configures the rf switches accordingly. There are 16 potential rf paths in the PM and 4 in the FM section. In all cases, the rf assembly consists of movable and fixed reeds and fixed contacts. The contact areas are hard anodized and sealed to prevent buildup of oxides. By careful design and process control, these contact areas provide capacitive, low-loss coupling across the frequency range of interest. It should be noted that there is no interruption of the rf during switching and the antenna switch is a "hot switch" design with the capability to switch a 175-watt rf signal. The rf head also includes mechanical contacts which are slaved to the rf contacts and provide status information on switch positions for telemetry and antenna management use.

The network signal processor (NSP) (fig. 26) essentially provides the interface between the S-band PM equipment and the other onboard systems. As shown, the forward link information is routed from the transponder receiver into a symbol synchronizer. When coding is in use, the NSP then routes the signal to the Viterbi decoder, and, in the case of secure data, the data are routed through the outboard COMSEC device. The information is then demultiplexed and demodulated or decoded as required. The signals are then routed to the users at the proper level and impedance. In the return link, the inverse functions are provided; onboard voice signals are received from the audio system and digitized in a delta modulation process using a Modified ABATE algorithm. The telemetry signals are then multiplexed with the voice. Then, depending on the operational mode, the signal is routed through the convolutional encoder or the COMSEC unit or both. The final processing is to convert from NRZ-L to biphase L and route the information at the proper level to the transponder modulator for rf transmission or to the ground-support equipment (GSE) data bus. The LRU has self-contained logic that recognizes the desired system configuration and internally controls the routing and processing.

The FM transmitter is frequency modulated by the output of the FM signal processor. The input modulates a 98.5-megahertz oscillator. This signal is then mixed with the eighth harmonic of a stabilized oscillator. The resulting 750-megahertz signal is filtered, amplified, and multiplied by 3 to drive the output power amplifier. The solid-state output amplifier produces a minimum of 10 watts rf. The companion FM signal processor (fig. 27) provides the interface function between the FM system and the various Orbiter data sources. Such signals as main engine data, television, and payload data are selected, level and impedance controlled, modulated on internally generated subcarriers, and provided as the modulating signal to the FM transmitter. An important function is the processing of high-speed telemetry playback data from the Orbiter recorders.

749
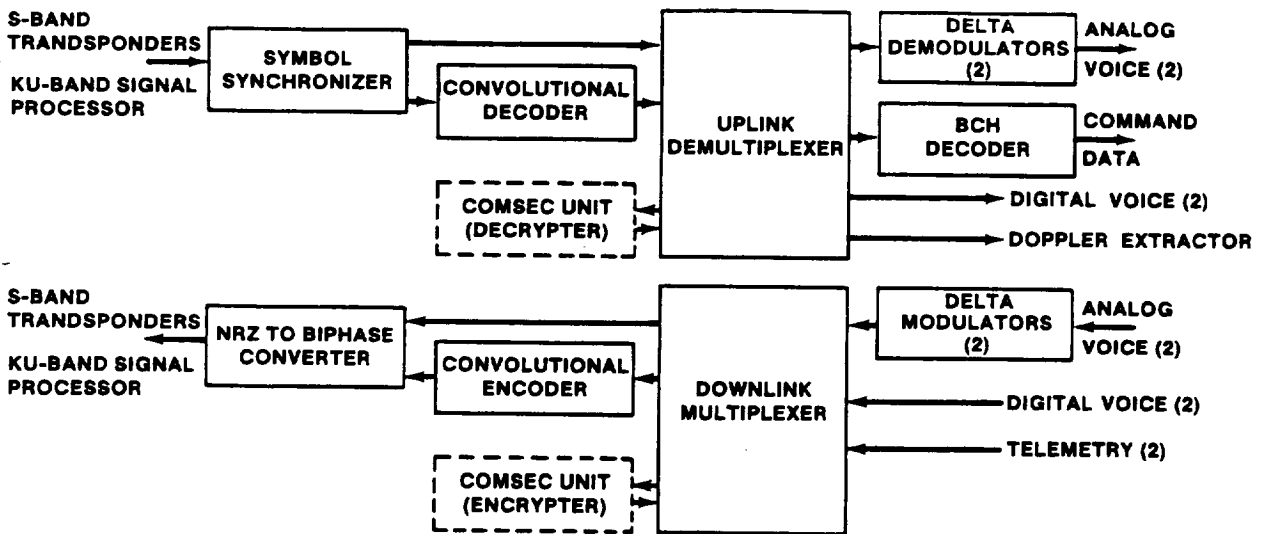
FIGURE 26.- NETWORK SIGNAL PROCESSOR FUNCTIONAL BLOCK DIAGRAM.
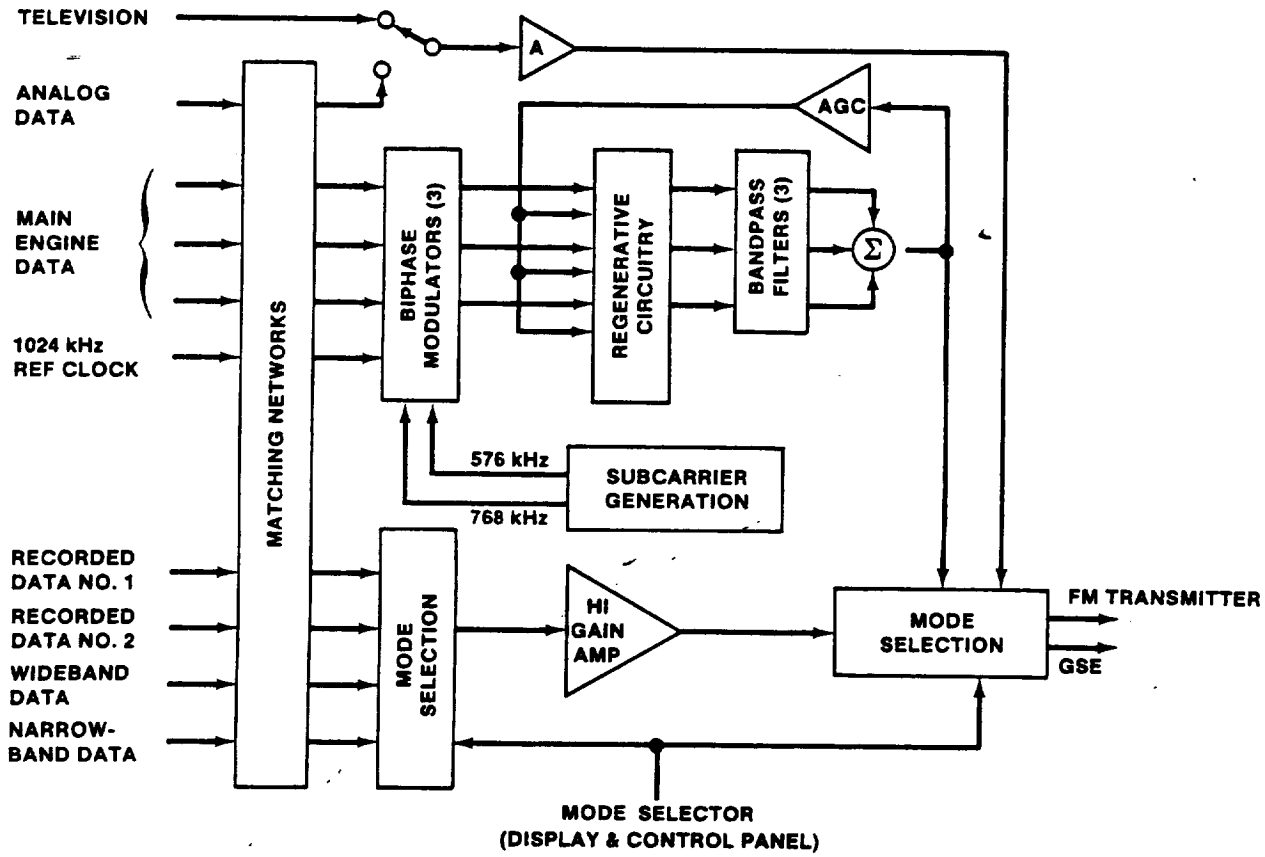
FIGURE 27.- FM SIGNAL PROCESSOR FUNCTIONAL BLOCK DIAGRAM.

GSTDN/TDRSS PERFORMANCE MARGINS

End-to-end data performance for communications or tracking links can be expressed in terms of a required SNR in an appropriate bandwidth at some point in the receiving system. For an analog chan-

750

nel, this may be the final demodulator output SNR or it may be the first demodulator input SNR which is necessary to provide the required final output SNR. For a digital channel, the SNR in the data-rate bandwidth at the bit detector input that is required for a given BEP is frequently used. For either analog or digital channels, the performance margin (or circuit margin) is the amount, in decibels, by which the calculated (or measured) SNR exceeds the required SNR at the chosen reference point in the receiving system. The required SNR (and thus the performance margin) can also be expressed in terms of the received signal-to-noise power spectral density ratio P_r/N_0.

Table 10 summarizes Shuttle S-band network performance margins for a representative selection of Orbiter and ground station/TDRSS modes. These margins reflect conservative, end-of-life parameter values but are not considered to be worst case in the sense of using worst case tolerances. The TDRSS margins reflect Orbiter antenna performance for an average 50-percent spherical coverage. The return link margins do not include any degradation due to ground-based rf interference.

TABLE 10.- SHUTTLE S-BAND PERFORMANCE MARGIN SUMMARY

	Configuration	Channel	Performance margin
	GSTDN-to-Orbiter uplink		
1.	GSTDN: 9.1 m ant; 2 kW xmtr ORB: Preamp bypass Both: On-orbit modulation, ranging off, high-data-rate mode, 270 n. mi. orbit	72 kbps data	45.7 dB (10^{-4} BEP)
2.	Same as 1, except ranging on	72 kbps data Ranging	42.9 dB (10^{-4} BEP) 54.8 dB (P_r/N_0 = 49.4 dB-Hz)
3.	GSTDN: 9.1 m ant; 2 kW xmtr ORB: Preamp in Both: Launch modulation, ranging on, high-data-rate mode, range = 460 n. mi.	72 kbps data Ranging	62.2 dB (10^{-4} BEP) 65.6 dB (P_r/N_0 = 49.4 dB-Hz)
	AF/SCF-to-Orbiter uplink		
	AF/SCF: 14 m ant; 1 kW xmtr ORB: Preamp bypass Both: High-data-rate mode, 225 n. mi. orbit	72 kbps data	40.4 dB (10^{-5} BEP)
	Orbiter-to-GSTDN PM downlink		
	GSTDN: 9.1 m ant; 140 K syst temp ORB: Power amp bypass, coherent mode Both: Ranging on, high-data-rate mode	192 kbps data Ranging	14.2 dB (10^{-4} BEP) 31.4 dB (P_r/N_0 = 53.5 dB-Hz)
	Orbiter-to-AF/SCF PM downlink		
	AF/SCF: 14 m ant; 220 K syst temp ORB: Power amp bypass, coherent mode Both: High-data-rate mode, 225 n. mi. orbit	192 kbps data	14.1 dB (10^{-5} BEP)

TABLE 10.- Concluded

Configuration	Channel	Performance margin
Orbiter-to-GSTDN FM downlink		
GSTDN: 9.1 m ant; 140 K syst temp		
Both: ?70 n. mi. orbit		
(1) Recorder playback	1024 kbps data	7.9 dB $(10^{-4}$ BEP)
(2) Main engine subcarriers	60 kbps data	8.1 dB $(10^{-4}$ BEP)
(3) Digital payload data	5 Mbps data	.1 dB $(10^{-4}$ BEP)
(4) Analog payload data	4 MHz data	1.1 dB (SNR = 13.5 dB)
(5) Television	3 MHz video	1.4 dB (SNR = 33.0 dB)
Orbiter-to-AF/SCF FM downlink		
AF/SCF: 14 m ant; 220 K syst temp, SGLS receiver		
Both: 225 n. mi. orbit		
(1) Recorder playback	960 kbps data	9.0 dB $(10^{-5}$ BEP)
(2) Digital payload data	256 kbps data	14.1 dB $(10^{-5}$ BEP)
TDRSS-to-Orbiter forward link		
(1) Low-data-rate data	32 kbps	2.1 dB $(10^{-4}$ BEP)
(2) High-data-rate data	72 kbps	-1.4 dB $(10^{-4}$ BEP)
Orbiter-to-TDRSS return link		
(1) Low-data-rate data	96 kbps	3.5 dB $(10^{-4}$ BEP)
(2) High-data-rate data	192 kbps	.5 dB $(10^{-4}$ BEP)

DATA/RANGING INTERFERENCE EFFECTS

Interchannel compatibility of the GSTDN/Orbiter data and ranging channels has been well demonstrated during the first Shuttle flights. However, earlier versions of the design had significant interference problems which were exposed in ESTL system performance verification testing at JSC. These initial-design problems and the resulting interference effects on link performance are described in the following paragraph.

The initial data/ranging design used a major ranging tone of 100 kilohertz instead of 500 kilohertz. Tests using nominal modulation indexes and the 100-kilohertz major tone resulted in unusable ranging data. Tests using nominal modulation and the 500-kilohertz major tone indicated degraded but acceptable ranging performance (25 meters compared to 10 meters specified range accuracy, 20 seconds average acquisition time, and 2 percent probability of incorrect acquisitions). Ranging test results using the 500-kilohertz major tone and worst case modulation indexes, however, were unacceptable (100 meters accuracy, 30 to 95 seconds acquisition time, and 30 to 40 percent probability of incorrect acquisition). Based on subsequent tests and analyses, the downlink data modulation index was reduced from 1.1 ± 10 percent radians to 0.55 ± 10 percent radians, providing good ranging performance (5 meters accuracy, 17 seconds acquisition time, and no incorrect acquisitions). Downlink data performance was degraded by 4.6 decibels as a result of the modulation index reduction, but performance margins for 10^{-4} BEP were still very high (+18 decibels for the low-power mode).

RADIOFREQUENCY COVERAGE ANALYSIS

Radiofrequency coverage analysis is to be distinguished from the closely related activity known as circuit margin analysis. Both deal with link performance assessment and prediction, but the latter is a generalized and limited assessment. It excludes the mission time-variable factors: spacecraft orientation and trajectory. Circuit margins are calculated for a fixed range or distance and, in the case of omnidirectional antennas, a nominal reference value of antenna gain and polarization. The rf coverage analysis, on the other hand, is keyed to mission time and spacecraft position and at-

titude and thus provides a dynamic analysis of the rf links as the spacecraft moves along its trajectory with ever-changing attitude and range to ground stations or the TDRSS. It is the only end-to-end rf link performance assessment that analyzes rf links in their real form, combining the mission-fixed and mission time-varying link characteristics.

Radiofrequency coverage analysis is also reiterative. It is repeated during early planning stages as mission changes or new inputs occur and, in fact, is itself sometimes the catalyst for trajectory and attitude changes. When a mission's final operational trajectory is released, a formal rf coverage report is published, giving performance predictions for that particular mission. After the mission, rf coverage postmission analysis addresses anomalies, assesses actual compared to expected rf link performance, and considers whether changes are needed to subsequent mission plans.

Figure 28 characterizes the rf coverage and performance analysis process (ref. 14). The basic characterization of the rf links is given by the familiar range equation

$$P_r = P_t \frac{G_t G_r c^2}{16\pi^2 R^2 f^2 L_c L_m} \tag{12}$$

where

P_r, P_t = received and transmitted signal power, respectively
G_r, G_t = receive and transmit antenna gain, respectively
f = frequency
R = range
c = speed of light
L_c = circuit losses (transmit and receive)
L_m = miscellaneous losses (pointing, polarization, etc.)
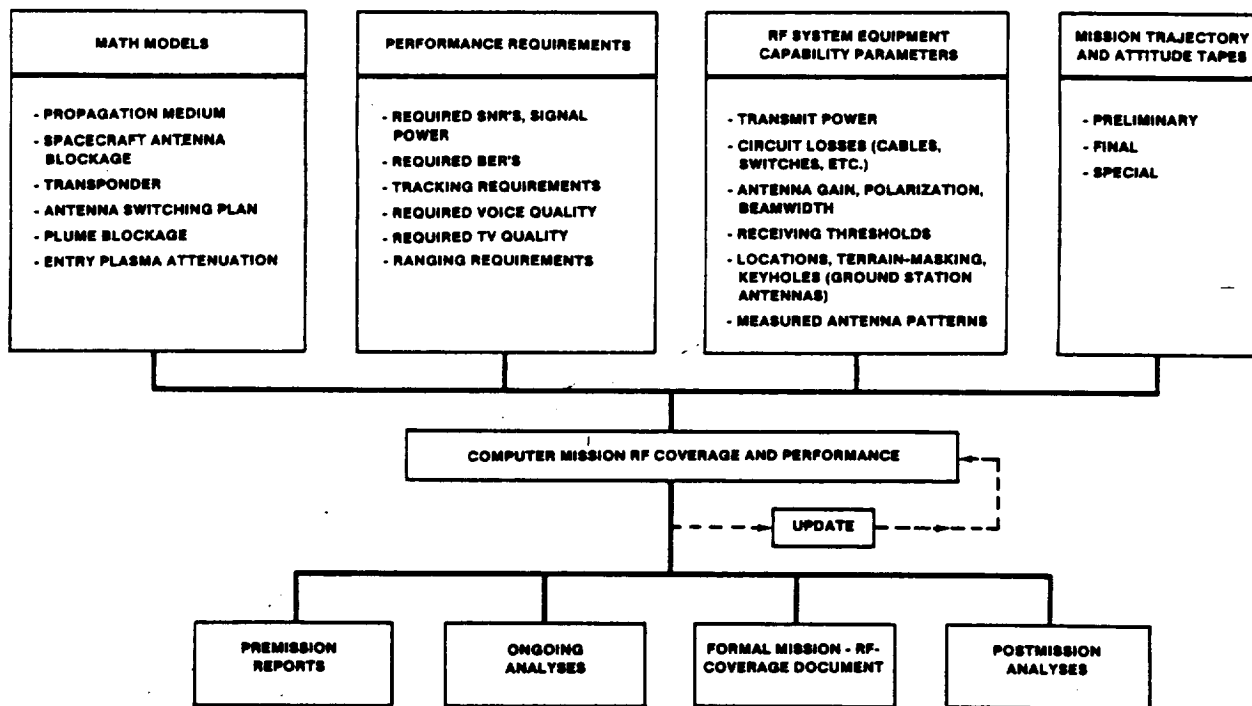

FIGURE 28.- RF COVERAGE AND PERFORMANCE ANALYSIS PROCESS.

With the Shuttle moving along its trajectory with changing attitude, its range and antenna gain (for omnidirectional antennas) are time variables and must be continuously computed as a function of time. The position and attitude at each instant is given by the state vector (position and velocity compo-

753

nents, X, Y, Z, Ẋ, Ẏ, Ż) and directional cosines, respectively. The Shuttle omnidirectional antennas generally receive a final reference set of measurements at the JSC antenna test range facility, whereas vehicle antenna blockage is usually modeled from physical structural measurements.

## MISSION PHASE CONSIDERATIONS

Ascent and descent mission phases have strict navigation requirements, and the Shuttle trajectory and attitude cannot be tailored to communication needs. With certain exceptions, on-orbit navigation requirements are more flexible and vehicle attitude (but not trajectory) can be planned to at least partly favor communications.

During ascent, Shuttle attitude relative to the Merritt Island (MIL) ground station changes rapidly; therefore, antenna gain of the S-band PM and FM antennas and hence the link signal strength varies considerably. There are four PM link antennas, one for each quadrant about the spacecraft. Switching can be manual but is normally automatic, initiated by onboard computer identification of which quadrant contains the line of sight.

As the Shuttle ascends and heads downrange, the radio links to MIL operate in the low-gain aft region and also in the solid rocket booster (SRB) exhaust plume. Figure 29 shows a typical plot of the S-band PM signal strength at MIL from the Shuttle, from lift-off until MIL loss of sight. The period when the line of sight with MIL passes through the plume is indicated on the graph. The signal strength during this period is much lower than shown because of plume attenuation (as much as 60 decibels has been observed) and also erratic because of phase distortion. Figure 30 is typical of the variation of the Shuttle-to-MIL line of sight during the ascent phase. Continuous communications with MIL cannot be assured when the line of sight is close to or within the dashed-box plume-blockage region. A decision was made in 1977 to locate a ground station at Ponce De Leon (PDL), somewhat north of the MIL site, so that its line of sight would be outside this blockage region. Shuttle missions have confirmed that MIL does lose communications during this period and that PDL is largely unaffected.
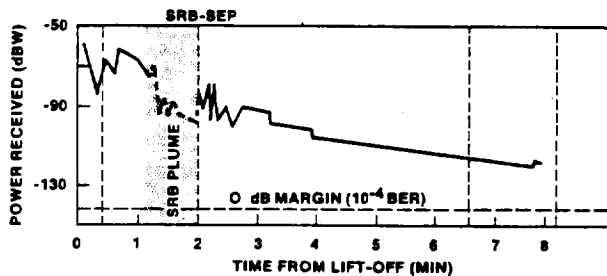
FIGURE 29.- ASCENT-PHASE PM SIGNAL STRENGTH, SHUTTLE TO MIL (TYPICAL).
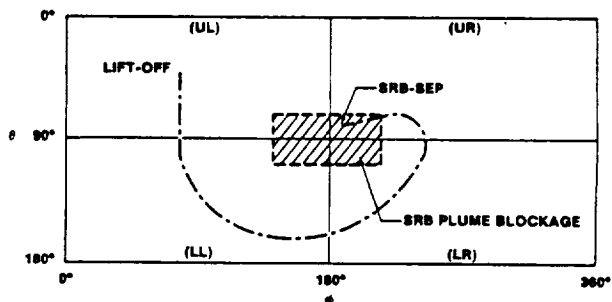
FIGURE 30.- ASCENT-PHASE LOOK ANGLES, SHUTTLE TO MIL (TYPICAL).

Circuit margin analysis for the S-band PM links between the Shuttle and the TDRS show 2 to 4 decibels margin when the line of sight lies in the main coverage region of the Shuttle S-band PM link antennas. During ascent, however, the line of sight from the Shuttle to the TDRS is in and out of the main coverage region (or the external tank/SRB blockage region) during the first few minutes and continuous communication by way of TDRS is highly unlikely until after the first 4 to 6 minutes as illustrated in figure 31. The MIL/PDL stations, on the other hand, are expected to have a strong signal from lift-off through about the first 7 to 8 minutes. Figure 32 illustrates the coverage using MIL/PDL for the first 8 minutes and TDRSS thereafter. The MIL/PDL/TDRS combination is the baseline projected when TDRS becomes operational.

During the descent phase, communications will again be through the S-band quads. Figure 33 illustrates the signal strength of the S-band Shuttle link to both TDRSS satellites, as predicted, using a typical descent trajectory for a landing at Edwards Air Force Base in California. Figure 33 encompasses the period from an altitude of 170 000 feet to an altitude of about 10 000 feet. The look angles are in and out of the fore and aft regions of the Shuttle, where the PM quad antennas have their lowest gain, as a result of large attitude excursions by the Orbiter as it dissipates excess energy. Reliable communications for descent, like ascent, probably will require a ground station assist to the TDRSS. Ground station links for descent are very strong, as has been demonstrated in missions to date, because of ground station proximity (compared to the TDRSS satellites being some 23 000 nautical miles farther away).
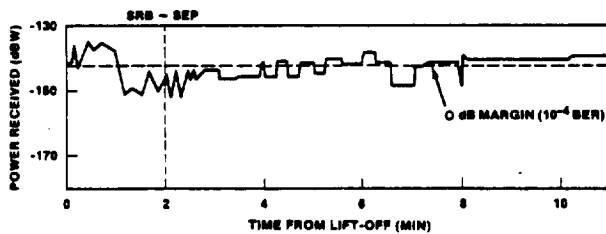
FIGURE 31.- ASCENT-PHASE PM SIGNAL STRENGTH, SHUTTLE TO TDRS EAST (TYPICAL).
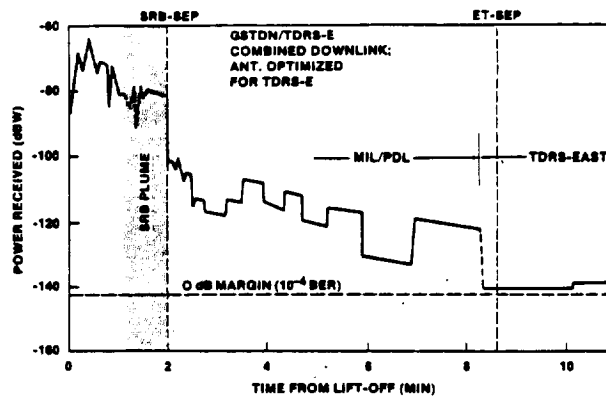
FIGURE 32.- ASCENT-PHASE GROUND STATION/SATELLITE COMPOSITE COVERAGE. PM SIGNAL STRENGTH, SHUTTLE TO MIL/PDL/TDRS EAST (TYPICAL).
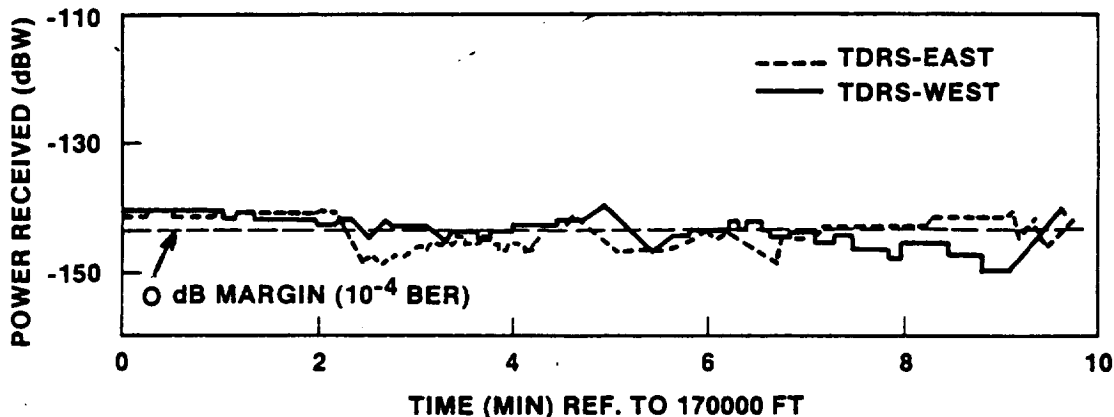
FIGURE 33.- DESCENT-PHASE PM SIGNAL STRENGTH, SHUTTLE TO TDRS EAST AND TDRS WEST (TYPICAL).

A communications "blackout" occurs during descent because of a plasma/shock sheath created by the Shuttle's high-speed entry into the Earth's atmosphere. The blackout has been extensively analyzed, but, because the sheath and its effects are not fully amenable to analytical methods, explicit analytical predictions should be treated only as preliminary estimates. Furthermore, results may be different for different missions since trajectory, velocity, and attitude all have an effect on sheath thickness, flow, and intensity. Also, since the thickness, flow, and intensity vary at different points around the vehicle, the amount of blackout likewise depends on which antenna is being used and the line-of-sight direction to the ground station (or TDRS).

Blackout for the Shuttle has been predicted to be only a "grayout." For example, the peak S-band signal attenuation is predicted to be on the order of 20 to 25 decibels compared to 100 decibels in the Apollo Program. The maximum effect is predicted to occur around 250 000 feet altitude or higher, decreasing to little or none by about 200 000 feet, which is before the Shuttle normally comes into view of descent-phase ground stations (typically approximately 180 000 feet). Hence, no blackout has been observed at these ground stations for missions to date. Because of the alternate landing at Northrup strip of STS-3, the Hawaii ground station had the Shuttle within line of sight and received signals briefly from about 290 000 feet to 250 000 feet, as did an advanced range instrumentation aircraft during STS-2 at about 210 000 feet. Although the data were not conclusive, there were indications that plasma attenuation on the order of 5 to 15 decibels was present during the STS-3 Hawaii pass.

REFERENCES

1. Viterbi, Andrews: Error Bounds for Convolutional Codes and Asymptotically Optimum Decoding Algorithms. IEEE Transactions On Information Theory, vol. IT-13, no. 2, Apr. 1967, pp. 260-269.

2. Abate, J. E.: Linear and Adaptive Delta Modulation. Proc. IEEE, vol. 55, Mar. 1967, pp. 298-308.

3. Shelling, Donald L.; et al.: Voice Encoding for Space Shuttle Using Adaptive Modulation. IEEE Transactions, vol. COM-26, Nov. 1978, pp. 1652-1659.

4. ESTL NASA Task 501 Orbiter/TDRSS S-Band Forward Link TDM System Verification Test Report. JSC-16689, Oct. 1980.

5. Batson, Bartus H.; Moorehead, Robert W.; et. al.: Simulation Results for the Viterbi Decoding Algorithm. NASA Technical Report, MSC-07027, July 1972.

6. Seyl, J. W.; and Kapell, M. H.: Applications of Spread Spectrum to the Shuttle Orbiter Communication System. Proceedings National Telecomm Conference, Dec. 1976.

7. Alem, Waddah K.: Spread Spectrum Acquisition and Tracking Performance for Shuttle Communication Links. IEEE Transactions, vol. COM-26, Nov. 1978, pp. 1689-1703.

8. Lindsey, W. C.: False Lock Phenomenon in the Shuttle S-Band PN Code Tracking Loop. LINCOM Corp. Report - TR-0382-1080 (NASA Contract NAS 9-16097), Mar. 1982.

9. Cubley, Dean H.: Antenna Development for the Space Shuttle Orbiter Vehicle. IEEE Transactions, vol. COM-26, Nov. 1978, pp. 1713-1722.

10. Wso, Kai T.; et al.: False Lock Performance of Shuttle Costas Loop Receivers. IEEE Transactions, vol. COM-26, Nov. 1978, pp. 1703-1712.

11. Novosad, Sidney; and Schmalz, Mark: An Automatic (Hands-off) Acquisition Technique for STS-1 S-Band PM Links. JSC-16981, Nov. 26, 1980.

12. Simon, Marvin K.: The Effects of Residual Carrier on Costas Loop Performance as Applied to the Space Shuttle Orbiter S-Band Link. IEEE Transactions on Communications, vol. COM-26, no. 11, Nov. 1978, pp. 1542-1548.

13. Seyl, J. W.; Smith, B. G.; and Batson, Bartus H.: Experimental Results for FSK Data Transmission System Using Discriminator Detection. Proceedings, National Telecomm Conference, Dec. 1976.

14. Loh, Yin-chung; and Porter, James A.: RF Coverage Analysis and Performance for Shuttle Communication Links. IEEE Transactions on Communications, vol. COM-26, no. 11, Nov. 1978, pp. 1745-1757.